

Weierstraß-Institut für Angewandte Analysis und Stochastik

im Forschungsverbund Berlin e.V.

Preprint

ISSN 0946 – 8633

Stochastic Spectral and Fourier-Wavelet Methods for Vector Gaussian Random Fields

Orazgeldi Kurbanmuradov¹, and Karl Sabelfeld^{2,3}

¹ Center for Phys. Math. Research
Turkmenian State University
Saparmyrat Turkmenbashy av. 31
744000 Ashgabad, Turkmenistan

² Weierstrass Institute for Applied
Analysis and Stochastics
Mohrenstraße 39
D – 10117 Berlin, Germany
E-Mail: sabelfel@wias-berlin.de

³ Institute of Computational Mathematics
and Mathematical Geophysics, Russian Acad. Sci.
Lavrentieva str.,6, 630090 Novosibirsk, Russia

No. 1082
Berlin 2005



1991 *Mathematics Subject Classification.* 65C05, 60F05, 60F10.

Key words and phrases. Randomized Spectral models, Fourier-Wavelet method, plane wave decomposition .

This work is supported partly by the grants: German DFG Grant 436 TUK 17/1/05, Russian RFBR Grant N 03-01-00914, and NATO Collaborative Linkage Grant CLG N 981426.

Edited by
Weierstraß-Institut für Angewandte Analysis und Stochastik (WIAS)
Mohrenstraße 39
10117 Berlin
Germany

Fax: + 49 30 2044975
E-Mail: preprint@wias-berlin.de
World Wide Web: <http://www.wias-berlin.de/>

Abstract

Randomized Spectral Models (RSM) and Randomized Fourier-Wavelet Models (FWM) for simulation of homogeneous Gaussian random fields based on spectral representations and plane wave decomposition of random fields are developed. Extensions of FWM to vector random processes are constructed. Convergence of the constructed Fourier-Wavelet models (in the sense of finite-dimensional distributions) under some general conditions on the spectral tensor is given. A comparative analysis of RSM and FWM is made by calculating Eulerian and Lagrangian statistical characteristics of a 3D isotropic incompressible random field through an ensemble and space averaging.

1 Introduction

Stochastic approach becomes more and more popular in all branches of science and technology, especially in problems where the data are highly irregular (in deterministic sense). As a rule, in such problems it is very difficult and expensive to carry out measurements to extract the desired data. As important examples we mention the turbulent flow simulation [32]), and construction of flows through porous media [17], [4]. The temporal and spatial scales of the input parameters in this class of problems are varying enormously, and the behaviour is very complicated, so that there is no chance to describe it deterministically. In the stochastic approach, one needs to know a few number of parameters, like the mean and correlation tensor, whose behaviour in time and space is much more regular, so that usually, it is easier to extract them through measurements.

In most applications, it is assumed that the random fields are Gaussian, or that they can be obtained by a functional transformation of Gaussian fields. Generally, it is very difficult to construct efficient simulation methods for inhomogeneous random fields even if they are Gaussian. Therefore, the most developed methods deal with homogeneous or quasi homogeneous random fields, i.e., the characteristic scales of the variations of the means of the field are considerably larger than the correlation scale. There are highly intensive studies and literature concerned with the simulation of homogeneous and quasi homogeneous random fields. We mention here only some publications dealing with the main simulation methods.

Important class of methods includes models based on spectral representations. It includes (1) Discrete Spectral Method (DSM) ([38]) which is simply a deterministic discrete approximation of the Fourier Stilties integral; (2) Randomized Spectral Method (RSM) ([21], [31], [36])) which is based on a randomized approximation of the same Fourier Stilties

integral; (3) Fourier-Wavelet Method (FWM) ([10], [12], [13]) is a different approximation of the Fourier Stilties integral based on reexpansion in a special family of orthogonal functions, and is obtained by an expansion of the Gaussian white noise in wavelet basis.

Another class of methods includes methods which deal with the expansions in the physical space, in the relevant system of orthonormal functions: (1) methods based on expansions in wavelet basis (WM) ([45], [40]), (2) Karhunen-Loeve expansion method (KLEM) ([39], [43]) based on the expansions in eigen functions of the correlation operator; note that it works also for inhomogeneous random fields. (3) Moving Averages Method (MAM) ([29]) based on the representation of the random field in the form of a convolution of a deterministic function (more precisely, a Fourier transform of a square root of the spectral function) with the Gaussian white noise in the physical space. We mention the Fast Fourier Transform Spectral Method (FFTSM) (e.g., see [35], [7]) which is a particular case of the Discrete Spectral Method whose nodes are chosen as a diadic mesh to apply further the Fast Fourier Method.

The Matrix Factorization Method (MFM) ([8],[37]) and Circulant Embedding Method (CEM)([9]) is based on the Holessky decomposition of the covariance matrix.

The methods listed above all have their advantages and disadvantages as well. For example, DSM, RSM, and MAM, are simple and convenient for implementation; they provide the possibility to calculate the values of the random field at some points on demand. But in multidimensional cases, DSM and MAM are less efficient. FFTSM is also simple for implementation, but it calculates the random field only on a diadic mesh and has therefore a disadvantage that the samples are periodic. Further, FWM and WM models are efficient for simulating multiscale processes but they are difficult in implementation.

The KLEM model is highly efficient but is not universal since it is necessary to solve the eigen-value problem for the correlation operator.

More details about the mentioned methods can be found in [10], [2], [15], [34], [22], [23] where also a comparative analysis of some methods is given. In particular, in [2], [10], RSM and FWM are compared by analysing a fractal random field with the spectral function $F(k) = k^{-\alpha}$ ($1 < \alpha < 3$), where the calculated structure function was compared with the exact result. The main conclusion is that to construct the samples of a multiscale random field with a fixed desired accuracy, the cost of RSM is considerably lower than that of FWM if $\lg(l_{max}/l_{min}) \leq 4$ where l_{min} and l_{max} are the minimal and maxiamal spatial scales of the random field, respectively. In [23] we have shown that a logarithmically uniform subdivision of the spectral space (we have introduced such a subdivision in [26]) when calculating two- and a few-point statistical characteristics of the fractal random field, the RSM is more efficient than FWM for all values of l_{max}/l_{min} . In particular, when calculating the structure function of a multiscale random field with $\alpha = -5/3$, $l_{max}/l_{min} = 10^{12}$ it was found that the cost of FWM was 12 times larger than that of RSM; results were obtained for 9 decades, with a fixed accuracy.

Up to now, we discussed the calculation of statistical characteristics by ensemble averaging over the samples constructed by the relevant method. In many practical problems (e.g., in underground hydrology) only data obtained through spatial averaging is at hand, for instance, statistical characteristics obtained by a spatial averages, or over a family of Lagrangian trajectories generated in one fixed sample of the field (e.g., see [5], [17]). If the random field is ergodic (which in practice is almost always true), then the ensemble

averages can be well approximated by the appropriate space averages. This is very important when a boundary value problem with random parameters is solved: then in contrast to the ensemble averaging, we have to solve the problem only once, and then make the relevant averaging over space. In practical calculations, to increase the efficiency, it is sometimes reasonable to combine both the space and ensemble averaging, e.g., see [27], [20]. The same technique is used also in simulation of turbulent transport [16], [41].

So we conclude that good ergodic properties of the constructed random field model are very important and desired in practical problems. In [23] we studied ergodic properties of RSM and FWM. Calculations of structure functions through ensemble and space averaging have shown that the ergodic properties of FWM are much better than that of RSM. So in RSM, to obtain a good approximation through space averaging, it is necessary to take many thousands of harmonics per each decade !. However this conclusion was made only for random processes (i.e., random fields depending on one scalar variable).

In the present paper we deal with an analogous comparative analysis of RSM and FWM for three-dimensional random fields. Since the cost of both methods is proportional to the number of decades of the simulated random field, $\lg(l_{max}/l_{min})$, it is not necessary to handle multi-scale random fields. In this paper we simulate a 3D isotropic incompressible random field whose longitudinal correlation function is exponential. In the comparative analysis we have also included a Stratified Randomized Fourier-Wavelet model (SRFWM), a new version of FWM we have introduced in this paper. We also generalized the FWM to vector random fields (we are aware only of papers dealing with FWM for scalar processes and isotropic fields, see [2], [10]-[14], [22]).

The article is organized as follows. In Section 2, we present the basic formulae for the discrete expansions of random fields (starting from its spectral representation) in orthonormal system of functions. In Section 3, we give the basics of the Fourier-Wavelet expansions, and the Wavelet expansions too, to stress the difference between these two representations. The randomization of spectral expansions is described in Section 4. In Section 5, the Fourier-Wavelet model for random processes is presented, with a study of the error when a finite number of terms is taken in the relevant series expansion. Here we compare the model with the original method published in [10]. In Section 6, we present an approach known as a plane wave decomposition of random fields, which suggests a general technique of random field simulation through samples of stochastic processes. We describe different versions (deterministic, randomized, and stratified randomized) for choosing the nodes in the stochastic integral representation through the plane wave decomposition. In Section 7, we present the simulation results for a 3D isotropic incompressible random field carried out by different versions of RSM and FWM. We compare the Eulerian longitudinal and transversal correlation functions, the Lagrangian correlation function of velocity, and the diffusion coefficient. All these statistical characteristics were calculated both by ensemble and space averaging. The main results are summarized in the Conclusion, and some technical details are included in Appendices A and B.

2 Discrete expansions related with the spectral representations of Gaussian random fields

2.1 Spectral representations

We deal in this paper with real-valued homogeneous Gaussian l -dimensional vector random fields $\mathbf{u}(\mathbf{x}) = (u_1(\mathbf{x}), \dots, u_l(\mathbf{x}))^T$, $\mathbf{x} \in \mathbb{R}^d$ with a given correlation tensor $B(\mathbf{r})$:

$$B_{ij}(\mathbf{r}) = \langle u_i(\mathbf{x} + \mathbf{r}) u_j(\mathbf{x}) \rangle, \quad i, j = 1, \dots, l, \quad (2.1)$$

or with the corresponding spectral tensor F :

$$F_{ij}(\mathbf{k}) = \int_{\mathbb{R}^d} e^{-i2\pi\mathbf{k}\cdot\mathbf{r}} B_{ij}(\mathbf{r}) d\mathbf{r}, \quad B_{ij}(\mathbf{r}) = \int_{\mathbb{R}^d} e^{i2\pi\mathbf{r}\cdot\mathbf{k}} F_{ij}(\mathbf{k}) d\mathbf{k}, \quad i, j = 1, \dots, l. \quad (2.2)$$

We will assume that the condition $\int_{\mathbb{R}^d} |B_{jj}(\mathbf{r})| d\mathbf{r} < \infty$ is satisfied which ensures that the spectral functions F_{ij} are uniformly continuous with respect to \mathbf{k} . Here B_{jj} is the trace of B , i.e., we use here and in what follows the summation convention under repeated indices. Note that a weaker assumption that B is squared integrable guarantees only the existence of the spectral tensor in the space L_2 .

Let $Q(\mathbf{k})$ be an $l \times n$ -matrix defined by

$$Q(\mathbf{k})Q^*(\mathbf{k}) = F(\mathbf{k}), \quad Q(-\mathbf{k}) = \bar{Q}(\mathbf{k}). \quad (2.3)$$

Here the star stands for the complex conjugate transpose which is equivalent to taking two operations, the transpose T , and the complex conjugation of each entry.

Then the spectral representation of the random field is written as follows (e.g., see [18], [32], [44])

$$\mathbf{u}(\mathbf{x}) = \int_{\mathbb{R}^d} e^{i2\pi\mathbf{k}\cdot\mathbf{x}} Q(\mathbf{k}) \mathbf{Z}(d\mathbf{k}) \quad (2.4)$$

where the column-vector $\mathbf{Z} = (Z_1, \dots, Z_n)^T$ is a complex-valued homogeneous n -dimensional white noise on \mathbb{R}^d with a unite variance and zero mean:

$$\langle \mathbf{Z}(d\mathbf{k}) \rangle = 0, \quad \langle Z_i(d\mathbf{k}_1) \bar{Z}_j(d\mathbf{k}_2) \rangle = \delta_{ij} \delta(\mathbf{k}_1 - \mathbf{k}_2) d\mathbf{k}_1 d\mathbf{k}_2 \quad (2.5)$$

satisfying the condition $\mathbf{Z}(-d\mathbf{k}) = \bar{\mathbf{Z}}(d\mathbf{k})$. Note that the last condition can be satisfied as follows. Let $\mathbf{Z} = (\mathbf{Z}_R + i\mathbf{Z}_I)/\sqrt{2}$ where \mathbf{Z}_R and \mathbf{Z}_I are independent homogeneous real-valued white n -dimensional vector noises with a unity variance and zero mean defined on the half space $[0, \infty) \times \mathbb{R}^{d-1}$. Now, we prolong the measures \mathbf{Z}_R and \mathbf{Z}_I on $(-\infty, 0) \times \mathbb{R}^{d-1}$ by $\mathbf{Z}_R(d\mathbf{k}) = \mathbf{Z}_R(-d\mathbf{k})$, and $\mathbf{Z}_I(d\mathbf{k}) = -\mathbf{Z}_I(-d\mathbf{k})$.

All these conditions ensure that the random field (2.4) has real-valued components.

There is a different spectral representation which we will use further. Let us introduce a complex random field

$$\mathbf{w}(\mathbf{x}) = \mathbf{u}_R(\mathbf{x}) + i\mathbf{u}_I(\mathbf{x}) = \int_{\mathbb{R}^d} e^{i2\pi\mathbf{k}\cdot\mathbf{x}} Q(\mathbf{k}) \mathbf{W}(d\mathbf{k}). \quad (2.6)$$

Here $\mathbf{W}(d\mathbf{k}) = \mathbf{W}_R(d\mathbf{k}) + i\mathbf{W}_I(d\mathbf{k})$ is an n -dimensional complex white noise where the real and imagine parts are two independent homogeneous white noises on the whole space \mathbb{R}^d with unit variance and zero mean. It is not difficult to see that $\mathbf{u}_R(\mathbf{x})$ and $\mathbf{u}_I(\mathbf{x})$ are independent Gaussian random fields both having the spectral tensor $F(\mathbf{k})$.

2.2 Series expansions

In this section, we deal with the expansions

$$\mathbf{u}(\mathbf{x}) = \sum_{\alpha \in \mathcal{A}} G_\alpha(\mathbf{x}) \xi_\alpha \quad (2.7)$$

where $G_\alpha(\mathbf{x})$ is a system of deterministic functions (or possibly matrices), ξ_α is a family of random variables (possibly vectors) \mathcal{A} is a countable (finite or not) index set.

Our purpose is to construct the system G_α and the family ξ_α so that the random field (2.7) has the desired spectral tensor (2.2).

2.2.1 Expansion with even complex orthonormal system

Let us choose the system of scalar functions $\varphi_\alpha(\mathbf{k})$ as a set of generally complex valued even functions ($\varphi_\alpha(-\mathbf{k}) = \bar{\varphi}_\alpha(\mathbf{k})$) which are orthonormal and complete in $L_2(\mathbb{R}^d)$ equipped with the scalar product $(f, g) = \int_{\mathbb{R}^d} f(\mathbf{k})\bar{g}(\mathbf{k}) d\mathbf{k}$:

$$(\varphi_\alpha, \varphi_\beta) = \int_{\mathbb{R}^d} \varphi_\alpha(\mathbf{k})\bar{\varphi}_\beta(\mathbf{k}) d\mathbf{k} = \delta_{\alpha\beta}, \quad \alpha, \beta \in \mathcal{A}, \quad (2.8)$$

where $\delta_{\alpha\beta}$ is the Kronecker symbol. Since $B_{jj}(0) = \int F_{jj}(\mathbf{k}) d\mathbf{k} < \infty$, and $QQ^* = F$, we conclude that all the entries of the matrix Q belong to $L_2(\mathbb{R}^d)$. Then, we expand $e^{i2\pi \mathbf{k} \cdot \mathbf{x}} Q(\mathbf{k})$ as a function of \mathbf{k} in the system of orthonormal functions $\varphi_\alpha(\mathbf{k})$:

$$e^{i2\pi \mathbf{k} \cdot \mathbf{x}} Q(\mathbf{k}) = \sum_{\alpha \in \mathcal{A}} G_\alpha(\mathbf{x}) \varphi_\alpha(\mathbf{k}), \quad G_\alpha(\mathbf{x}) = \int_{\mathbb{R}^d} e^{i2\pi \mathbf{k} \cdot \mathbf{x}} Q(\mathbf{k}) \bar{\varphi}_\alpha(\mathbf{k}) d\mathbf{k}. \quad (2.9)$$

We now substitute this representation in (2.4), and obtain the expansion (2.7) with

$$\xi_\alpha = \int_{\mathbb{R}^d} \varphi_\alpha(\mathbf{k}) \mathbf{Z}(d\mathbf{k}), \quad \alpha \in \mathcal{A}. \quad (2.10)$$

Note that by the construction and the assumptions made, the random vectors ξ_α and the functions $G_\alpha(\mathbf{x})$ are all real valued. Notice also that ξ_α are mutually independent standard Gaussian random vectors since

$$\langle \xi_\alpha \xi_\beta^* \rangle = \mathbb{I} \int_{\mathbb{R}^d} \varphi_\alpha(\mathbf{k}) \bar{\varphi}_\beta(\mathbf{k}) d\mathbf{k} = \mathbb{I} \delta_{\alpha\beta},$$

where \mathbb{I} is a $n \times n$ identity matrix.

Thus we have constructed an expansion of type (2.7) with independent Gaussian random vectors.

2.2.2 Expansion with real orthonormal system.

Let us construct another expansion starting from a set of orthonormal scalar real valued functions $g_\alpha(\mathbf{x})$ complete in $L_2(\mathbb{R}^d)$:

$$(g_\alpha, g_\beta) = \int_{\mathbb{R}^d} g_\alpha(\mathbf{x}) g_\beta(\mathbf{x}) d\mathbf{x} = \delta_{\alpha\beta} .$$

Then,

$$\mathbf{u}(\mathbf{x}) = \sum_{\alpha \in \mathcal{A}} g_\alpha(\mathbf{x}) \boldsymbol{\xi}_\alpha \quad (2.11)$$

where the family of random column-vectors of dimension l is defined by

$$\boldsymbol{\xi}_\alpha = \int \mathbf{u}(\mathbf{x}) g_\alpha(\mathbf{x}) d\mathbf{x}. \quad (2.12)$$

Substitution of the representation (2.2) in (2.12) yields

$$\boldsymbol{\xi}_\alpha = \int_{\mathbb{R}^d} \hat{g}_\alpha(-\mathbf{k}) Q(\mathbf{k}) \mathbf{Z}(d\mathbf{k}), \quad \hat{g}_\alpha(\mathbf{k}) = \int_{\mathbb{R}^d} e^{-i2\pi \mathbf{k}\cdot\mathbf{x}} g_\alpha(\mathbf{x}) d\mathbf{x} . \quad (2.13)$$

Note that $\boldsymbol{\xi}_\alpha$ are real valued Gaussian random column-vectors of dimension l ; these vectors are generally correlated, in contrast to the family (2.10).

2.3 Complex valued orthogonal expansions

A different expansion can be obtained if we expand $e^{i2\pi \mathbf{k}\cdot\mathbf{x}} Q(\mathbf{k})$ in (2.6) in the form of (2.9) where φ_α is a set of arbitrary (possibly not even) orthonormal complex valued functions complete in $L_2(\mathbb{R}^d)$, while $G_\alpha(\mathbf{x})$ and the family $\boldsymbol{\xi}_\alpha$ are defined in (2.9) and (2.10), respectively. This gives

$$\begin{aligned} \mathbf{u}_R(\mathbf{x}) &= \sum_{\alpha} \left(G_\alpha^{(R)}(\mathbf{x}) \boldsymbol{\xi}_\alpha^{(R)} - G_\alpha^{(I)}(\mathbf{x}) \boldsymbol{\xi}_\alpha^{(I)} \right) , \\ \mathbf{u}_I(\mathbf{x}) &= \sum_{\alpha} \left(G_\alpha^{(R)}(\mathbf{x}) \boldsymbol{\xi}_\alpha^{(I)} - G_\alpha^{(I)}(\mathbf{x}) \boldsymbol{\xi}_\alpha^{(R)} \right) , \end{aligned} \quad (2.14)$$

where

$$G_\alpha(\mathbf{x}) = G_\alpha^{(R)}(\mathbf{x}) + i G_\alpha^{(I)}(\mathbf{x}), \quad \boldsymbol{\xi}_\alpha = \boldsymbol{\xi}_\alpha^{(R)} + i \boldsymbol{\xi}_\alpha^{(I)} .$$

Analogously, we can generalize the expansion (2.11) to the general complex valued case. Let $g_\alpha(\mathbf{x})$ be an arbitrary complete system of complex valued orthonormal functions in $L_2(\mathbb{R}^d)$, and let $\boldsymbol{\xi}_\alpha$ be a family of random column-vectors defined in (2.13). Then,

$$\begin{aligned} \mathbf{u}_R(\mathbf{x}) &= \sum_{\alpha} \left(g_\alpha^{(R)}(\mathbf{x}) \boldsymbol{\xi}_\alpha^{(R)} - g_\alpha^{(I)}(\mathbf{x}) \boldsymbol{\xi}_\alpha^{(I)} \right) , \\ \mathbf{u}_I(\mathbf{x}) &= \sum_{\alpha} \left(g_\alpha^{(R)}(\mathbf{x}) \boldsymbol{\xi}_\alpha^{(I)} + g_\alpha^{(I)}(\mathbf{x}) \boldsymbol{\xi}_\alpha^{(R)} \right) , \end{aligned} \quad (2.15)$$

where

$$g_\alpha(\mathbf{x}) = g_\alpha^{(R)}(\mathbf{x}) + i g_\alpha^{(I)}(\mathbf{x}), \quad \boldsymbol{\xi}_\alpha = \boldsymbol{\xi}_\alpha^{(R)} + i \boldsymbol{\xi}_\alpha^{(I)} .$$

3 Wavelet expansions

In this section we consider an important example of expansions based on even orthogonal systems described in subsection 1.2.1. For simplicity we present here the one-dimensional case, $d = 1$.

Our goal is to construct the expansion of a homogeneous Gaussian vector random process $\mathbf{u}(x) = (u_1(x), \dots, u_l(x))^T$, $x \in \mathbb{R}$ with a given spectral tensor $F(k)$.

Again, we assume that $F = Q Q^*$, where $Q(\mathbf{k})$ is $l \times n$ -dimensional matrix satisfying the condition $Q(-k) = \bar{Q}(k)$. The orthonormal system of functions φ_α is constructed as follows.

Let us introduce the notations: $\phi(x)$ and $\psi(x)$, $x \in \mathbb{R}$ are orthonormal scaling and wavelet functions, respectively, and

$$\phi_{mj}(x) = 2^{m/2} \phi(2^m x - j), \quad \psi_{mj}(x) = 2^{m/2} \psi(2^m x - j), \quad (3.1)$$

where $m, j = \dots, -2, -1, 0, 1, 2, \dots$. It is known (e.g., see [3], [19]) that the system of functions

$$\{\phi_{m_0j}\}_{j=-\infty}^{\infty}, \quad \left\{ \{\psi_{mj}\}_{j=-\infty}^{\infty}, \quad m \geq m_0 \right\} \quad (3.2)$$

is, for an arbitrary fixed integer m_0 , a complete set of orthonormal functions in $L_2(\mathbb{R})$, and moreover, by Parseval equality, the relevant Fourier transforms of these functions

$$\{\hat{\phi}_{m_0j}\}_{j=-\infty}^{\infty}, \quad \left\{ \{\hat{\psi}_{mj}\}_{j=-\infty}^{\infty}, \quad m \geq m_0 \right\} \quad (3.3)$$

compose also a complete set of orthonormal functions in $L_2(\mathbb{R})$.

3.1 Fourier-wavelet expansions

Thus we choose, as the family φ_α , the system of functions (3.3).

From (2.9) and (2.7) we find that

$$\mathbf{u}(x) = \sum_{j=-\infty}^{\infty} G_{m_0j}^{(\phi)}(x) \boldsymbol{\xi}_j + \sum_{m=m_0}^{\infty} \sum_{j=-\infty}^{\infty} G_{mj}^{(\psi)}(x) \boldsymbol{\xi}_{mj}, \quad (3.4)$$

where $\boldsymbol{\xi}_j, \boldsymbol{\xi}_{mj}$ is a family of mutually independent standard real valued Gaussian random vectors of dimension n , and $G_{mj}^{(\phi)}(x), G_{mj}^{(\psi)}(x)$ are $l \times n$ -dimensional matrices defined by

$$G_{mj}^{(\phi)}(x) = \int_{-\infty}^{\infty} e^{i2\pi kx} Q(k) \bar{\phi}_{mj}(k) dk, \quad G_{mj}^{(\psi)}(x) = \int_{-\infty}^{\infty} e^{i2\pi kx} Q(k) \bar{\psi}_{mj}(k) dk.$$

It is clear that

$$\hat{\phi}_{mj}(k) = 2^{-m/2} e^{-i2\pi k j 2^{-m}} \hat{\phi}(2^{-m} k), \quad \hat{\psi}_{mj}(k) = 2^{-m/2} e^{-i2\pi k j 2^{-m}} \hat{\psi}(2^{-m} k). \quad (3.5)$$

Now we can define the analog of G_α by substituting $\bar{\varphi}_\alpha(k)$ in (2.9) with these expressions, which yields

$$\begin{aligned}
G_{mj}^{(\phi)}(x) &= \int_{-\infty}^{\infty} e^{i2\pi kx} Q(k) \hat{\phi}_{mj}(-k) dk = \int_{-\infty}^{\infty} e^{-i2\pi kx} \bar{Q}(k) \hat{\phi}_{mj}(k) dk \\
&= \int_{-\infty}^{\infty} e^{-i2\pi kx} \bar{Q}(k) 2^{-m/2} e^{-i2\pi k j 2^{-m}} \hat{\phi}(2^{-m} k) dk \\
&= \int_{-\infty}^{\infty} e^{-i2\pi k'(2^m x + j)} 2^{m/2} \bar{Q}(2^m k') \hat{\phi}(k') dk' .
\end{aligned} \tag{3.6}$$

Analogously,

$$G_{mj}^{(\psi)}(x) = \int_{-\infty}^{\infty} e^{-i2\pi k'(2^m x + j)} 2^{m/2} \bar{Q}(2^m k') \hat{\psi}(k') dk' . \tag{3.7}$$

For convenience, we define

$$\begin{aligned}
\mathcal{F}_m^{(\phi)}(y) &= \int_{-\infty}^{\infty} e^{-i2\pi ky} 2^{m/2} \bar{Q}(2^m k) \hat{\phi}(k) dk, \\
\mathcal{F}_m^{(\psi)}(y) &= \int_{-\infty}^{\infty} e^{-i2\pi ky} 2^{m/2} \bar{Q}(2^m k) \hat{\psi}(k) dk,
\end{aligned} \tag{3.8}$$

hence

$$G_{m_0 j}^{(\phi)}(x) = \mathcal{F}_{m_0}^{(\phi)}(2^{m_0} x + j) , \quad G_{mj}^{(\psi)}(x) = \mathcal{F}_m^{(\psi)}(2^m x + j) , \tag{3.9}$$

and finally,

$$\mathbf{u}(x) = \sum_{j=-\infty}^{\infty} \mathcal{F}_{m_0}^{(\phi)}(2^{m_0} x + j) \boldsymbol{\xi}_j + \sum_{m=m_0}^{\infty} \sum_{j=-\infty}^{\infty} \mathcal{F}_m^{(\psi)}(2^m x + j) \boldsymbol{\xi}_{mj} . \tag{3.10}$$

3.2 Wavelet expansion

In this section we deal with the expansion of the type (2.11) and use the scaling and wavelet functions (3.1), as the orthonormal system G_α . Thus the expansion reads

$$\mathbf{u}(x) = \sum_{j=-\infty}^{\infty} \phi_{m_0 j}(x) \boldsymbol{\xi}_{m_0 j}^{(\phi)} + \sum_{m=m_0}^{\infty} \sum_{j=-\infty}^{\infty} \psi_{mj}(x) \boldsymbol{\xi}_{mj}^{(\psi)} , \tag{3.11}$$

where $\boldsymbol{\xi}_{m_0 j}^{(\phi)}$ and $\boldsymbol{\xi}_{mj}^{(\psi)}$ is a set of Gaussian column-vectors of dimension n defined as follows:

$$\boldsymbol{\xi}_{mj}^{(\phi)} = \int_{-\infty}^{\infty} Q(k) \hat{\phi}_{mj}(-k) \mathbf{Z}(dk) = \int_{-\infty}^{\infty} Q(k) 2^{-m/2} e^{i2\pi k j 2^{-m}} \bar{\phi}(2^{-m} k) \mathbf{Z}(dk) , \tag{3.12}$$

and analogously,

$$\boldsymbol{\xi}_{mj}^{(\psi)} = \int_{-\infty}^{\infty} Q(k) 2^{-m/2} e^{i2\pi k j 2^{-m}} \bar{\psi}(2^{-m} k) \mathbf{Z}(dk) . \quad (3.13)$$

Note that in contrast to the Fourier wavelet expansions, here the random vectors $\boldsymbol{\xi}_{mj}^{(\phi)}$ and $\boldsymbol{\xi}_{mj}^{(\psi)}$ are correlated, and in particular, in calculations one needs the following correlations:

$$\langle \boldsymbol{\xi}_{mj_1}^{(\phi)} (\boldsymbol{\xi}_{mj_2}^{(\phi)})^T \rangle = 2^{-m} \int_{-\infty}^{\infty} e^{i2\pi k(j_1-j_2)} |\hat{\phi}(2^{-m} k)|^2 F(k) dk , \quad (3.14)$$

$$\langle \boldsymbol{\xi}_{mj_1}^{(\phi)} (\boldsymbol{\xi}_{mj_2}^{(\psi)})^T \rangle = 2^{-m} \int_{-\infty}^{\infty} e^{i2\pi k(j_1-j_2)} \left(\bar{\phi}(2^{-m} k) \hat{\psi}(2^{-m} k) \right) F(k) dk , \quad (3.15)$$

$$\langle \boldsymbol{\xi}_{mj_1}^{(\psi)} (\boldsymbol{\xi}_{mj_2}^{(\psi)})^T \rangle = 2^{-m} \int_{-\infty}^{\infty} e^{i2\pi k(j_1-j_2)} |\hat{\psi}(2^{-m} k)|^2 F(k) dk . \quad (3.16)$$

It is worth noting that in the expansion (3.11), a biorthogonal system of wavelet functions can be used, see [40].

3.3 Moving averages

Let $F(\mathbf{k})$ be an $l \times l$ -dimensional spectral tensor of a random field, and $Q(\mathbf{k})$ be an $l \times n$ -dimensional complex-valued matrix satisfying (2.3). Since obviously $B_{jj}(0) = \int F_{jj}(\mathbf{k}) d\mathbf{k} < \infty$, we see by (2.3) that the entries of the matrix are squared integrable, i.e., $Q(\mathbf{k}) \in L_2(\mathbb{R}^d)$. Therefore the $l \times n$ -dimensional matrix

$$G(\mathbf{x}) = \int_{\mathbb{R}^d} e^{i2\pi \mathbf{k}\mathbf{x}} Q(\mathbf{k}) d\mathbf{k} \quad (3.17)$$

is well defined, with real valued square integrable entries.

We define now an l -dimensional homogeneous Gaussian random field

$$\mathbf{u}(\mathbf{x}) = \int_{\mathbb{R}^d} G(\mathbf{x} - \mathbf{y}) \mathbf{W}(d\mathbf{y}) \quad (3.18)$$

where $\mathbf{W}(d\mathbf{y}) = (W_1(d\mathbf{y}), \dots, W_n(d\mathbf{y}))^T$, and $W_i(d\mathbf{y})$, $i = 1, \dots, n$ are real valued independent homogeneous Gaussian white noises in \mathbb{R}^d with unite variance and zero mean. Then the random field (3.18) has the spectral tensor $F(\mathbf{k})$. Indeed,

$$\begin{aligned} \langle \mathbf{u}(\mathbf{x} + \mathbf{r}) \mathbf{u}^T(\mathbf{x}) \rangle &= \left\langle \int_{\mathbb{R}^d} G(\mathbf{x} + \mathbf{r} - \mathbf{y}) \mathbf{W}(d\mathbf{y}) \left(\int_{\mathbb{R}^d} G(\mathbf{x} - \mathbf{y}) \mathbf{W}(d\mathbf{y}) \right)^T \right\rangle \\ &= \int_{\mathbb{R}^d} G(\mathbf{x} + \mathbf{r} - \mathbf{y}) G^T(\mathbf{x} - \mathbf{y}) d\mathbf{y} = \int_{\mathbb{R}^d} G(\mathbf{z} + \mathbf{r}) G^T(\mathbf{z}) d\mathbf{z} \end{aligned}$$

Taking the Fourier transformation of the right-hand side we get

$$\begin{aligned} \int_{\mathbb{R}^d} e^{-i2\pi\mathbf{k}\mathbf{r}} d\mathbf{r} \int_{\mathbb{R}^d} G(\mathbf{z} + \mathbf{r}) G^T(\mathbf{z}) d\mathbf{z} &= \int_{\mathbb{R}^d} e^{-i2\pi\mathbf{k}(\mathbf{r}+\mathbf{z})} G(\mathbf{r} + \mathbf{z}) d(\mathbf{r} + \mathbf{z}) \int_{\mathbb{R}^d} e^{i2\pi\mathbf{k}\mathbf{z}}, G^T(\mathbf{z}) d\mathbf{z} \\ &= \int_{\mathbb{R}^d} e^{-i2\pi\mathbf{k}\mathbf{x}}, G^T(\mathbf{x}) d\mathbf{x} \overline{\left(\int_{\mathbb{R}^d} e^{-i2\pi\mathbf{k}\mathbf{z}} G^T(\mathbf{z}) d\mathbf{z} \right)} = Q(\mathbf{k})Q^*(\mathbf{k}) = F(\mathbf{k}). \end{aligned}$$

4 Randomized spectral models

A straightforward evaluation of the stochastic integral (2.4) is based on the Riemann sums calculation with fixed cells (see, e.g. [38], [35]). The integral is approximated by a finite sum

$$\mathbf{u}(\mathbf{x}) \approx \sum_{i=1}^n \left[\cos(2\pi\mathbf{k}_i \cdot \mathbf{x})\boldsymbol{\xi}_i + \cos(2\pi\mathbf{k}_i \cdot \mathbf{x})\boldsymbol{\eta}_i \right]$$

where \mathbf{k}_i are deterministic nodes in the Fourier space, $\boldsymbol{\xi}_i$ and $\boldsymbol{\eta}_i$ are Gaussian random vectors with zero mean and relevant covariance. Efficient calculation of the above sum is usually carried out by the fast Fourier transform which assumes that the nodes are chosen uniformly. It should be mentioned that this scheme suffers from an artificial periodicity in the scale of $1/\Delta k$ where Δk is the integration step in the Fourier space.

In Randomized models, the nodes are chosen at random, with an appropriate probability distribution so that the model has the desired correlation structure. We mention by passing that this model is free from the above mentioned artificial periodicity.

4.1 Randomized spectral models defined through stochastic integrals.

Let us consider an l -dimensional random field $\mathbf{u}(\mathbf{x})$, $\mathbf{x} \in \mathbb{R}^d$ defined by the stochastic integral [18]:

$$\mathbf{u}(\mathbf{x}) = \int_{\mathbb{R}^d} \mathcal{H}(\mathbf{x}, \mathbf{k}) \mathbf{W}(d\mathbf{k}), \quad (4.1)$$

where (1) $\mathcal{H} : \mathbb{R}^d \times \mathbb{R}^{d_1} \rightarrow \mathcal{C}^{l \times n}$ is a matrix such that $\mathcal{H}(\mathbf{x}, \cdot) \in L_2(\mathbb{R}^{d_1})$ for each $\mathbf{x} \in \mathbb{R}^d$; (2) $\mathbf{W}(\cdot) = \mathbf{W}_R(\cdot) + i\mathbf{W}_I(\cdot)$, where $\mathbf{W}_R(\cdot)$ and $\mathbf{W}_I(\cdot)$ are two independent n -dimensional homogeneous Gaussian white noises on \mathbb{R}^{d_1} with unit variance. Here \mathcal{C} is the set of complex numbers.

Let us describe the randomized evaluation of the stochastic integral (4.1). Let $p : \mathbb{R}^{d_1} \rightarrow [0, \infty)$ be a probability density on \mathbb{R}^{d_1} : $\int p(\mathbf{k}) d\mathbf{k} = 1$, and let $\mathbf{k}_1, \dots, \mathbf{k}_{n_0}$ are independent equally distributed random points in \mathbb{R}^{d_1} with the density $p(\mathbf{k})$. Assume that $\boldsymbol{\zeta}_1, \dots, \boldsymbol{\zeta}_{n_0}$ is a family of mutually independent standard Gaussian complex random vectors of dimension n (i.e., $\boldsymbol{\zeta}_j = \boldsymbol{\xi}_j + i\boldsymbol{\eta}_j$ with independent, n -dimensional real valued standard

Gaussian random vectors $\boldsymbol{\xi}_i$ and $\boldsymbol{\eta}_i$). Then the random field

$$\mathbf{u}_{n_0}(\mathbf{x}) = \frac{1}{\sqrt{n_0}} \sum_{j=1}^{n_0} \frac{1}{\sqrt{p(\mathbf{k}_j)}} \mathcal{H}(\mathbf{x}, \mathbf{k}_j) \boldsymbol{\zeta}_j \quad (4.2)$$

has the same correlation tensor as $\mathbf{u}(\mathbf{x})$, provided $p(\mathbf{k})$ satisfies the condition

$$p(\mathbf{k}) > 0, \quad \text{if } \exists \mathbf{x} \in \mathbb{R}^d : \mathcal{H}(\mathbf{x}, \mathbf{k}) \neq 0.$$

In practical calculations, to guarantee an equal presentation of different spectral regions, one uses a stratified randomization technique (e.g., see [31],[36]). Let us describe it briefly. Let $\{\Delta_i\}_{i=1}^N$ be a subdivision of the spectral space \mathbb{R}^d : $\mathbb{R}^d = \cup_{i=1}^N \Delta_i$, and $\Delta_i \cap \Delta_j = \emptyset$ if $i \neq j$. This generates the representation of the random field $\mathbf{u}(\mathbf{x})$ as a sum of independent random fields:

$$\mathbf{u}(\mathbf{x}) = \sum_{i=1}^N \mathbf{u}_i(\mathbf{x}), \quad \mathbf{u}_i(\mathbf{x}) = \int_{\Delta_i} \mathcal{H}(\mathbf{x}, \mathbf{k}) \mathbf{W}(d\mathbf{k}).$$

Let $p_i : \Delta_i \rightarrow [0, \infty)$ ($i = 1, \dots, N$) be a probability density on Δ_i : $\int_{\Delta_i} p(\mathbf{k}) d\mathbf{k} = 1$ satisfying the condition $p_i(\mathbf{k}) > 0$, for $\mathbf{k} \in \Delta_i$ if $\exists \mathbf{x} \in \mathbb{R}^d : \mathcal{H}(\mathbf{x}, \mathbf{k}) \neq 0$. Then using the randomized representation for $\mathbf{u}_i(\mathbf{x})$ we get a stratified randomization model for $\mathbf{u}(\mathbf{x})$:

$$\mathbf{u}_{N,n_0}(\mathbf{x}) = \sum_{i=1}^N \frac{1}{\sqrt{n_0}} \sum_{j=1}^{n_0} \frac{1}{\sqrt{p_i(\mathbf{k}_{ij})}} \mathcal{H}(\mathbf{x}, \mathbf{k}_{ij}) \boldsymbol{\zeta}_{ij}, \quad (4.3)$$

where $\{\mathbf{k}_{ij}\}_{j=1}^{n_0} \subset \Delta_i$, $i = 1, \dots, N$ are mutually independent random points such that for fixed i the random points \mathbf{k}_{ij} , $j = 1, \dots, n_0$ are all distributed with the same density $p_i(\mathbf{k})$, and $\boldsymbol{\zeta}_{ij}$, $i = 1, \dots, N$; $j = 1, \dots, n_0$ are mutually independent, and independent of $\{\mathbf{k}_{ij}\}_{j=1}^{n_0}$ $i = 1, \dots, N$ family of n -dimensional complex valued standard Gaussian random variables.

By the construction, for any N and n_0 , the random field $\mathbf{u}_{N,n_0}(\mathbf{x})$ has the same correlation tensor as that of $\mathbf{u}(\mathbf{x})$. As the Central Limit Theorem says, by increasing n_0 (N fixed) the field $\mathbf{u}_{N,n_0}(\mathbf{x})$ is convergent to a gaussian random field (e.g., see [1],[24], [25]). So the stratified randomization model $\mathbf{u}_{N,n_0}(\mathbf{x})$ can be considered as an approximation to $\mathbf{u}(\mathbf{x})$.

4.2 Stratified RSM for homogeneous random fields

Let now $\mathbf{u}(\mathbf{x})$, $\mathbf{x} \in \mathbb{R}^d$ be a homogeneous l -dimensional Gaussian random field with the spectral tensor $F(\mathbf{k})$, $\mathbf{k} \in \mathbb{R}^d$, and let $Q(\mathbf{k})$ be an $l \times n$ -dimensional matrix satisfying the condition $Q(\mathbf{k})Q^*(\mathbf{k}) = F(\mathbf{k})$, $\mathbf{k} \in \mathbb{R}^d$. Then due to the spectral representation (2.6), the real and imaginary parts, $\mathbf{u}_R(\mathbf{x})$ and $\mathbf{u}_I(\mathbf{x})$ of the complex-valued field $\mathbf{w}(\mathbf{x})$ are two independent copies of the random field $\mathbf{u}(\mathbf{x})$. The field $\mathbf{w}(\mathbf{x})$ can be obviously represented (in view of (2.6)), as a stochastic integral (4.1) with the kernel $\mathcal{H}(\mathbf{x}, \mathbf{k}) = e^{i2\pi\mathbf{x}\cdot\mathbf{k}}Q(\mathbf{k})$. Therefore, the relevant stratified randomization model has the form

$$\mathbf{w}_{N,n_0}(\mathbf{x}) = \sum_{i=1}^N \frac{1}{\sqrt{n_0}} \sum_{j=1}^{n_0} \frac{e^{i2\pi\mathbf{x}\cdot\mathbf{k}_{ij}}}{\sqrt{p_i(\mathbf{k}_{ij})}} Q(\mathbf{k}_{ij}) \boldsymbol{\zeta}_{ij}. \quad (4.4)$$

with the conditions on the densities p_i written as $p_i(\mathbf{k}) > 0$ for $\mathbf{k} \in \Delta_i$ if $\max_{mr} |q_{mr}(\mathbf{k})| > 0$ (where $Q = (q_{mr})$). Taking the real part of (4.4) we get the stratified randomization model of the original real-valued random field $\mathbf{u}(\mathbf{x})$:

$$\mathbf{u}_{N,n_0}(\mathbf{x}) = \sum_{i=1}^N \frac{1}{\sqrt{n_0}} \sum_{j=1}^{n_0} \frac{1}{\sqrt{p_i(\mathbf{k}_{ij})}} \left\{ \left[Q'(\mathbf{k}_{ij}) \cos \theta_{ij} - Q''(\mathbf{k}_{ij}) \sin \theta_{ij} \right] \boldsymbol{\xi}_{ij} + \left[Q''(\mathbf{k}_{ij}) \cos \theta_{ij} + Q'(\mathbf{k}_{ij}) \sin \theta_{ij} \right] \boldsymbol{\eta}_{ij} \right\}. \quad (4.5)$$

Here $\theta_{ij} = 2\pi \mathbf{k}_{ij} \cdot \mathbf{x}$, $\{\mathbf{k}_{ij}\}$, $i = 1, \dots, N; j = 1, \dots, n_0$ are the same as in (4.3), and $\boldsymbol{\xi}_{ij}$, $\boldsymbol{\eta}_{ij}$, $i = 1, \dots, N; j = 1, \dots, n_0$ is a family of mutually independent and independent of the set $\{\mathbf{k}_{ij}\}$ n -dimensional real-valued standard Gaussian random variables.

5 Fourier-wavelet models

In the numerical implementation of (3.10) we have to: (1) choose the scaling and wavelet functions, (2) evaluate the coefficients (3.8), and (3) find a reasonable choice of the cut-off parameters m_0 and m_1 in the approximations:

$$\sum_{j=-\infty}^{\infty} \mathcal{F}_{m_0}^{(\phi)}(2^{m_0}x + j) \boldsymbol{\xi}_j \simeq \sum_{j=-b_0+[2^{m_0}x]}^{b_0+[2^{m_0}x]} \mathcal{F}_{m_0}^{(\phi)}(2^{m_0}x + j) \boldsymbol{\xi}_j, \quad (5.1)$$

$$\sum_{m=m_0}^{\infty} \sum_{j=-\infty}^{\infty} \mathcal{F}_m^{(\psi)}(2^m x + j) \boldsymbol{\xi}_{mj} \simeq \sum_{m=m_0}^{m_1} \sum_{j=-b_1+[2^m x]}^{b_1+[2^m x]} \mathcal{F}_m^{(\psi)}(2^m x + j) \boldsymbol{\xi}_{mj} \quad (5.2)$$

where $[a]$ stands for the integer part of a , and $b_0 = b_0(m_0)$, $b_1 = b_1(m)$ are such integers that supports of the functions $\mathcal{F}_{m_0}^{(\phi)}$ and $\mathcal{F}_m^{(\psi)}$ belong essentially to the intervals $[-b_0, b_0]$ and $[-b_1, b_1]$, respectively. We will deal here with a scalar random process $u(x)$, $x \in \mathbb{R}$. Extensions to vector random processes is straightforward.

5.1 Meyer wavelet functions

The Meyer wavelet functions $\phi(x)$ and $\psi(x)$ are defined by their Fourier transforms (e.g., see [6]):

$$\phi(x) = \int_{-\infty}^{\infty} e^{i2\pi kx} \hat{\phi}(k) dk, \quad \psi(x) = \int_{-\infty}^{\infty} e^{i2\pi kx} \hat{\psi}(k) dk, \quad (5.3)$$

where

$$\hat{\phi}(k) = \begin{cases} 1 & |k| \leq 1/3, \\ \cos[\frac{\pi}{2}\nu(3|k| - 1)], & 1/3 \leq |k| \leq 2/3 \\ 0, & \text{otherwise} \end{cases} \quad (5.4)$$

$$\hat{\psi}(k) = \begin{cases} e^{-i\pi k} \sin[\frac{\pi}{2}\nu(3|k| - 1)], & 1/3 \leq |k| \leq 2/3 \\ e^{-i\pi k} \cos[\frac{\pi}{2}\nu(\frac{3}{2}|k| - 1)], & 2/3 \leq |k| \leq 4/3 \\ 0, & \text{otherwise.} \end{cases} \quad (5.5)$$

Here $\nu(x)$ is a smooth function satisfying the following conditions: $\nu(x) \equiv 0$ for $x \leq 0$, $\nu(x) \equiv 1$ for $x \geq 1$, and $\nu(x) + \nu(1 - x) = 1$ for $0 < x < 1$. As an example of such a function, we consider a function $\nu(x) = \nu_p(x)$ depending on a positive parameter p (see [10]):

$$\nu_p(x) = \frac{4^{p-1}}{p} \left\{ [x - x_0]_+^p + [x - x_p]_+^p + 2 \sum_{j=1}^{p-1} (-1)^j [x - x_j]_+^p \right\},$$

where $x_j = (1/2)[\cos(((p-j)/p)\pi) + 1]$, and $[a]_+ = \max(a, 0)$. The function ν_p is $p - 1$ times continuously differentiable, therefore, choosing p sufficiently large, we can make the functions $\hat{\phi}$ and $\hat{\psi}$ smooth enough.

5.2 Evaluation of the coefficients $\mathcal{F}_m^{(\phi)}$ and $\mathcal{F}_m^{(\psi)}$.

Here we give some technical details on the calculation of the functions (3.8) which in our case reads

$$f_m(\xi) = \int_{-4/3}^{4/3} e^{-2\pi i k \xi} g(k) dk \quad (5.6)$$

where $g(k) = 2^{m/2} F^{1/2} (2^m k) \hat{\phi}(k)$ and $g(k) = 2^{m/2} F^{1/2} (2^m k) \hat{\psi}(k)$ for $\mathcal{F}_m^{(\phi)}$ and $\mathcal{F}_m^{(\psi)}$, respectively.

We calculate this function on the grid of points $\xi_j = -\frac{N}{2}\Delta\xi + (j-1)\Delta\xi$, $j = 1, \dots, N$, where N is an even number, and $\Delta\xi \geq 0$ is the grid step. In order to evaluate the truncated sums appearing in the Fourier-wavelet representation (3.7), we must choose $N\Delta\xi/2 \geq b$.

We approximate the integral (5.6) by a Riemann sum:

$$f_m(\xi_j) = \int_{-a}^a e^{-2\pi i k \xi} g(k) dk \simeq \sum_{l=1}^N \Delta k e^{-2\pi i k_l \xi_j} g(k_l) \quad (5.7)$$

where

$$k_l = -a + (l - 1/2)\Delta k, \quad l = 1, \dots, N; \quad \Delta k = \frac{2a}{N}.$$

We use the same number of points $N = 2^r$ (where r is some positive integer) to discretize the integral as we have done in representing $f_m(\xi)$ in physical space, so that we can apply the discrete fast Fourier transform. We also clearly need the cut-off in the integral in (5.7) to satisfy $a > 4/3$ (with $g(k)$ set to zero whenever evaluated for $|k| > 4/3$). Finally, the

use of the fast Fourier transform requires the steps in physical and wavenumber space be related through $\Delta\xi\Delta k = 1/N$. Indeed, simple transformations then yield

$$\begin{aligned}\xi_j k_l &= \left[-\frac{N}{2}\Delta\xi + (j-1)\Delta\xi \right] [-a + (l-1/2)\Delta k] \\ &= \frac{N-1}{4} - \frac{j-1}{2} \left(1 - \frac{1}{N}\right) - \frac{l-1}{2} + \frac{(j-1)(l-1)}{N},\end{aligned}\quad (5.8)$$

hence

$$f_m(\xi_j) \simeq \exp \left\{ \pi i (j-1) \left(1 - \frac{1}{N}\right) \right\} \sum_{l=1}^N G_l \exp \left\{ -2\pi i \frac{(j-1)(l-1)}{N} \right\}, \quad (5.9)$$

where

$$G_l = \Delta k g(k_l) \exp \left\{ -2\pi i \left[\frac{N-1}{4} - \frac{l-1}{2} \right] \right\},$$

which is in the form of a discrete Fourier transform.

The constraints imposed on the discretization of the integral (5.7) to obtain an expression amenable to fast Fourier transform imply the following sequence of choosing parameters. First a bandwidth value b is chosen according to the desired accuracy in the Fourier-wavelet representation (3.7). Then a spatial resolution $\Delta\xi$ for $f_m(\xi)$ is selected, either according to the grid spacing h on a prespecified set of evaluation points or such that $f_m(\xi)$ can be calculated accurately enough by interpolation from the computed values. (In any event, we must have $\Delta\xi < 3/8$). Next, a binary power $N = 2^r$ is chosen large enough so that $2b/N \leq \Delta\xi$. Then we set $a = \frac{1}{2\Delta\xi}$, and discretize the integral (5.7) with step size $\Delta k = 2a/N = 1/(N\Delta\xi)$.

5.3 Cut-off parameters

In practice, we use the approximation to $u(x)$:

$$u^{(FW)}(x) = \sum_{j=-b_0+\lfloor 2^{m_0}x \rfloor}^{b_0+\lfloor 2^{m_0}x \rfloor} \mathcal{F}_{m_0}^{(\phi)}(2^{m_0}x+j) \xi_j + \sum_{m=m_0}^{m_1} \sum_{j=-b_1+\lfloor 2^m x \rfloor}^{b_1+\lfloor 2^m x \rfloor} \mathcal{F}_m^{(\psi)}(2^m x+j) \xi_{mj}. \quad (5.10)$$

Recall that the parameters $b_0 = b_0(m_0)$ and $b_1 = b_1(m)$ are chosen from the criterion that the supports of the functions $\mathcal{F}_{m_0}^{(\phi)}$ and $\mathcal{F}_m^{(\psi)}$ belong essentially to the intervals $[-b_0, b_0]$ and $[-b_1, b_1]$, respectively.

Let us first suggest general arguments to the choice of parameters m_0 and m_1 . Theoretically, m_0 can be arbitrarily, and for a fixed m_1 , it would be reasonable to take the value of m_0 large enough since the cost per sample is proportional to $m_1 - m_0 + 1$. However practical calculations show that an important criterion for the choice of m_0 is that the value 2^{m_0} is comparable with k_0 , a characteristic wave number scale. This characteristic scale could be defined for instance as a value k_0 , for which the integrals $\int_0^{k_0} F(k) dk$ and

$\int_{k_0}^{\infty} F(k) dk$ are compared in the order of magnitude. It turns out that for values of m_0 for

which 2^{m_0} is essentially larger than k_0 , the dependence of $b_0 = b_0(m_0)$ on m_0 is exponential (see below), hence the cost of simulation is then increasing. When choosing the parameter m_1 one should remember that in the approximation of $u(x)$ by (5.10) the contributions of random harmonics with wave numbers from $k \in \mathbb{R} : |k| \geq 2^{m_1}$ are not taken into account. Therefore, to simulate accurately the random field in the interval (l_{min}, l_{max}) , the value of m_1 should be taken so that $2^{m_1} > 1/l_{min}$.

Thus suppose these arguments have helped us to choose some values of m_0 and m_1 . The next question then which arises naturally is the quantitative criterion of the approximation quality. (5.10). It is clear that for Gaussian processes, the main criterion is to have a good accuracy in evaluation of the correlation function. Therefore, the correlation function of $u^{(FW)}$ should well approximate the true correlation function $B(r) = \langle u(x+r)u(x) \rangle$ in an interval (l_{min}, l_{max}) depending on the problem to be solved. In what follows we assume that this interval is given. Thus with the fixed values of parameters m_0 and m_1 , the error of our approximation for the random field (5.10) is defined by

$$\varepsilon(m_0, m_1) = \sup_{l_{min} \leq r \leq l_{max}} |B(r) - B^{(FW)}(r)|, \quad (5.11)$$

where $B^{(FW)}(r) = \langle u^{(FW)}(x+r)u^{(FW)}(x) \rangle$. The random numbers ξ_j and ξ_{mj} in (5.10) are mutually independent, hence

$$\begin{aligned} B^{(FW)}(r) &= \sum_{j: |j| \vee |j - \lfloor 2^{m_0} x \rfloor| \leq b_0} \mathcal{F}_{m_0}^{(\phi)}(2^{m_0} r + j) \mathcal{F}_{m_0}^{(\phi)}(j) \\ &+ \sum_{m=m_0}^{m_1} \sum_{j: |j| \vee |j - \lfloor 2^m x \rfloor| \leq b_0} \mathcal{F}_m^{(\psi)}(2^m r + j) \mathcal{F}_m^{(\psi)}(j), \end{aligned} \quad (5.12)$$

here $a \vee b = \max\{a, b\}$. The cost to calculate the value of the random field $u^{(FW)}$ in one point is proportional to

$$T(m_0, m_1) = b_0(m_0) + \sum_{m=m_0}^{m_1} b_1(m). \quad (5.13)$$

Proposition 1 Assume that a spectral function $F(k)$ satisfies the condition (9.4) for some $s > 0$, and the function Q belongs to the Nikolskiĭ-Besov space $B_{1\infty}^\rho(\mathbb{R})$, $\rho > 1/2$. Then the following estimation is true:

$$\sup_{x \in \mathbb{R}} \sup_{r \in \mathbb{R}} |B(r) - \langle u^{(FW)}(x+r)u^{(FW)}(x) \rangle| \leq \frac{C_s}{4^{m_1} s} + \frac{C'_{m_0 \rho}}{b_0^{2\rho-1}(m_0)} + \sum_{m=m_0}^{m_1} \frac{C''_{m \rho}}{b_1^{2\rho-1}(m)}, \quad (5.14)$$

with the relevant constants C_s , $C'_{m_0 \rho}$ and $C''_{m \rho}$ depending on F , $\hat{\phi}$, and $\hat{\psi}$.

Proof. The proof is given in Appendix B

This estimation provides a justification for the construction of Fourier-wavelet approximations. Indeed, (5.14) shows that the right hand side of this estimation can be made arbitrarily small by a successive choice of the parameters. For example, we could first take some value of m_0 , then choose $b_0(m_0)$ so that the second term in the right hand side is small enough. Then choose m_1 so that the first term is small, and finally, choose $b_1(m)$, $m = m_0, \dots, m_1$ so that the last sum in (5.14) is small.

Unfortunately this approach cannot be practically used since it is difficult to calculate the coefficients C_s , C'_{m_0l} and C''_{ml} . In addition, the estimation (5.14) may be crude, then the described choice of parameters may be not the best one. Therefore in practice, we would recommend to use a direct estimation of $\sup_{r \in R} |B(r) - B^{(FW)}(r)|$ starting from (5.12).

5.4 Choice of parameters

In this section we discuss some aspects of the practical choice of the parameters of our model. First we the influence of the parameters m_0 and b_0 on the accuracy of approximation. So let us consider the behaviour of $\mathcal{F}_m^{(\phi)}(y)$ under the change of m . By the definitions (3.8) and (5.4) of the functions $\mathcal{F}^{(\phi)}$ and $\hat{\phi}$ it follows that for large negative values of m

$$\begin{aligned} \mathcal{F}_m^{(\phi)}(y) &= \int_{-2/3}^{2/3} e^{-i2\pi ky} 2^{m/2} Q(2^m k) \hat{\phi}(k) dk \\ &\approx \int_{-2/3}^{2/3} e^{-i2\pi ky} 2^{m/2} Q(0) \hat{\phi}(k) dk = 2^{m/2} Q(0) \phi(-y) \end{aligned} \quad (5.15)$$

provided $Q(k)$ is continuous at the point zero. It implies, for such values of m , the function $\mathcal{F}^{(\phi)}(y)$ behaves analogous to the scaling function $\phi(y)$ (which decreases as $|y|^{-p}$ as $|y| \rightarrow \infty$, where p is a parameter characterizing the smoothness of the function $\hat{\phi}$ such that $\hat{\phi} \in B_{1\infty}^p(\mathbb{R})$, see Appendix 2, Lemma 2).

For simplicity, and for the sake of a clear presentation, let us assume that $F(k) = 0$ if $|k| \geq k_*$, for same $k_* > 0$. Then for positive numbers m such that $2^m/3 \geq k_*$

$$\begin{aligned} \mathcal{F}_m^{(\phi)}(y) &= \int_{-1/3}^{1/3} e^{-i2\pi ky} 2^{m/2} Q(2^m k) dk + \int_{1/3 \leq |k| \leq 2/3} e^{-i2\pi ky} 2^{m/2} Q(2^m k) \hat{\phi}(k) dk \\ &= \int_{-\infty}^{\infty} e^{-i2\pi k 2^{-m} y} 2^{-m/2} Q(k) dk = 2^{-m/2} G(2^{-m} y). \end{aligned} \quad (5.16)$$

Hence with the increase of m , the effective support of the function $\mathcal{F}_m^{(\phi)}$ is expanded exponentially. Our experience says that such a broadening may happen in more general case when the support of the spectral function is not compact. For illustration, we show in Figure 1 the plots of the functions $\mathcal{F}_m^{(\phi)}(y)$ for different values of m , for $F(k) = 2/(1 + (2\pi k)^2)$ (see the left panel) and $F(k) = e^{-(\pi k)^2}$ (right panel).

So it suggests that the parameter m_0 should be chosen so that at $m = m_0$, the exponential broadening of the support of $\mathcal{F}_m^{(\phi)}$ is not yet happened. This implies the condition $2^{m_0} \leq k_0$, where k_0 is a characteristic wave number scale. For these values of m_0 the width of the support of $\mathcal{F}_{m_0}^{(\phi)}$ is practically independent of m_0 (recall that for $m \rightarrow -\infty$ the support width is defined by the function ϕ , in view of (5.15)) As a reasonable approximation we can put $b_0 = 10$.

Let us analyse the behaviour of $\mathcal{F}_m^{(\psi)}(y)$ for different values of m . The main difference between this function and the function $\mathcal{F}_m^{(\phi)}$ is that $\mathcal{F}_m^{(\psi)}$ is determined by the values of $Q(k)$ for $2^m/3 \leq |k| \leq 2^{(m+2)}/3$; while $\mathcal{F}_m^{(\phi)}$ depends on the values of $Q(k)$, $|k| \leq 2^{(m+1)}/3$.

Let us see what is the influence of this difference. Take an example of a spectrum $F(k)$ which for $|k| \geq k_0$ has the form

$$F(k) = C_F |k|^{-\alpha}, \quad |k| \geq k_0 \quad (5.17)$$

for some $k_0 > 0$ and $\alpha > 1$. Then, for $2^m/3 \geq k_0$, we conclude by the definitions (3.8) and (5.5) of the functions $\mathcal{F}^{(\psi)}$ and $\hat{\psi}$, respectively that for $m \geq \log_2(3k_0)$

$$\mathcal{F}_m^{(\psi)}(y) = \int_{1/3 \leq |k| \leq 4/3} e^{-i2\pi ky} 2^{m/2} Q(2^m k) \hat{\psi}(k) dk = 2^{-\frac{m}{2}(\alpha-1)} C_F^{1/2} A_\alpha(y), \quad (5.18)$$

where

$$A_\alpha(y) = \int_{1/3 \leq |k| \leq 4/3} e^{-i2\pi ky} |k|^{-\frac{\alpha}{2}} \hat{\psi}(k) dk.$$

It follows from this equality that the support of $\mathcal{F}_m^{(\psi)}$ is not broadening as m increases. Our experience shows that this property holds for many different spectral functions $F(k)$. We illustrate it in Figure 2 where $\mathcal{F}_m^{(\psi)}(y)$ for $F(k) = 2/(1 + (2\pi k)^2)$ (the left panel) and $F(k) = e^{-(\pi k)^2}$ (right panel) are presented. It is seen that for both spectral functions, $\mathcal{F}_m^{(\psi)}(y)$ are practically defined on $-10 \leq y \leq 10$. So we put $b_1 = 10$ for any m .

Thus when the values of b_0 and b_1 , are fixed, we can study the dependence of the Fourier-wavelet model on m_0 and m_1 . As an example, let us consider the case $F(k) = 2/(1 + (2\pi k)^2)$ with the relevant correlation function $B(r) = \exp(-r)$. Since $k_0 \simeq 1$, we can put $m_0 = 0$ (recall that 2^{m_0} should be of order k_0). In the first two rows of the Table 1 the dependence of the error (5.11) on m_1 is given, for the fixed value $m_0 = 0$, and l_{min} and l_{max} are chosen as $l_{min} = 0$ and $l_{max} = 5$.

It is seen that the error is rapidly decreasing with m_1 , and for $m_1 = 3$ it is about 0.0121.

In this example, we have compared our Fourier-wavelet model (5.10) with the Fourier-wavelet model [10] which can be obtained by ignoring the first sum in (5.10).

Note that the choice of m_0 in the model [10] is more difficult.

In the last two rows of the Table 1 we show the error $\tilde{\varepsilon}(m_0, m_1)$ of the model [10], for different values of m_0 , for fixed $m_1 = 3$. The cost of calculation of $u^{(FW)}$ is proportional to $m_1 - m_0$ (provided b_0 and b_1 do not depend on m), so the results of Table 1 show that in this example, the cost of the method [10] is more than two times larger than that of the model (5.10).

In all the above calculations we have fixed the parameters' values as $b_0 = b_1 = 10$. Let us study now the dependence of the error of the model (5.10) on the parameters b_0 and b_1 .

For the case of $F(k) = 1/(1 + (2\pi k)^2)$ we have reached the accuracy $\varepsilon(0, 6) = 0.01$ with $b_0 = b_1 = 5$, and $\varepsilon(0, 6) = 0.0029$ was obtained with $b_0 = b_1 = 6$. This shows that the values $b_0 = b_1 = 10$ we recommended are in this case slightly overestimated.

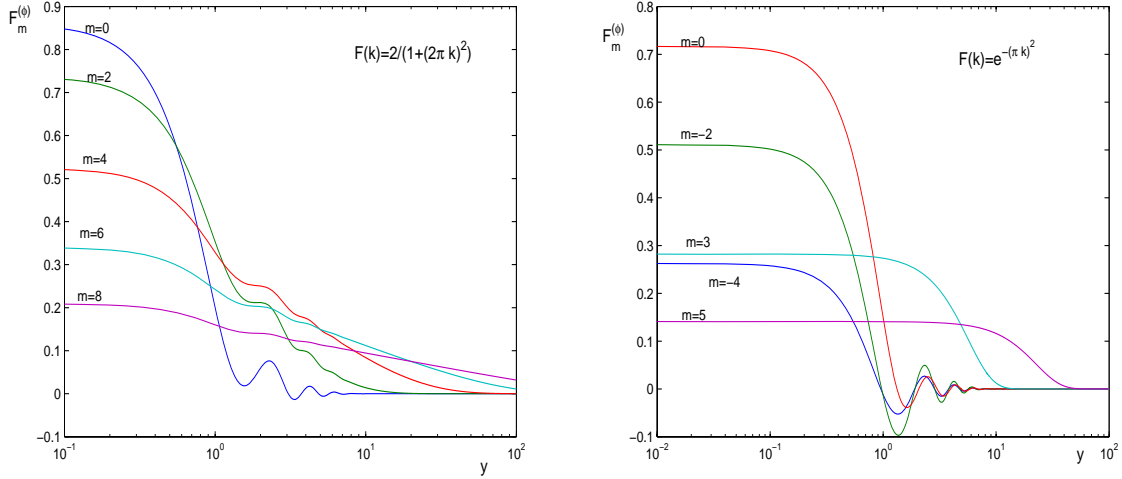


Figure 1: $\mathcal{F}_m^{(\phi)}(y)$ as a function of y , for different values of m . Left panel: $F(k) = \frac{2}{1+(2\pi k)^2}$; Right panel: $F(k) = e^{-(\pi k)^2}$.

We have also studied the error $\varepsilon(m_0, 6)$ for the model (5.10) for different values of m_0 . We have fixed $b_1 = 10$, and the parameter $b_0 = b_0(m_0)$ was varying dependent on m_0 in such a way that $\varepsilon(m_0, 6) \simeq 0.01$.

The computations give: $b_0(0) = 5$, $b_0(1) = 7$, and then, $b_0(m_0)$ is exponentially increasing as $b_0(m_0 + 1) = 7 \cdot 2^{m_0}$, $m_0 \geq 0$. Hence, the cost of evaluation of the field (5.10) in one point is proportional to $T(m_0, 6) \simeq 7 \cdot 2^{m_0-1} + 10(m_1 - m_0 + 1)$ (see (5.13)). If we choose b_0 to ensure $\varepsilon(m_0, 6) \simeq 0.003$, then $b_0(0) = 6$, $b_0(1) = 9$, and $b_0(m_0 + 1) = 9 \cdot 2^{m_0}$, $m_0 \geq 0$. This shows that the cost is exponentially increasing with m_0 .

m_1	1	2	3	4	5	6	7
$\varepsilon(0, m_1)$	0.0455	0.0233	0.0121	0.0068	0.0041	0.0029	0.0024
m_0	-3	-4	-5	-6	-7	-8	-9
$\tilde{\varepsilon}(m_0, 3)$	0.2714	0.1464	0.0789	0.0476	0.0303	0.0217	0.0124

Table 1: The errors of the Fourier-wavelet models, for different values of m_0 and m_1 . $F(k) = 1/(1 + (2\pi k)^2)$, $l_{min} = 0$, $l_{max} = 5$.

Remarks on vector processes. For vector processes $\mathbf{u}(x) = (u_1(x), \dots, u_l(x))^T$, $x \in \mathbb{R}$ ($l > 1$) the FW model is constructed analogously to the scalar case, as we got (5.10) from (3.10) by taking a finite number of terms. The following generalization of the Proposition 1 can be given.

Proposition 2 Assume that a spectral tensor $F(k)$ satisfies the condition

$$\int_{-\infty}^{\infty} spF(k)(1 + |k|^2)^s dk < \infty \quad (spF = F_{jj}),$$

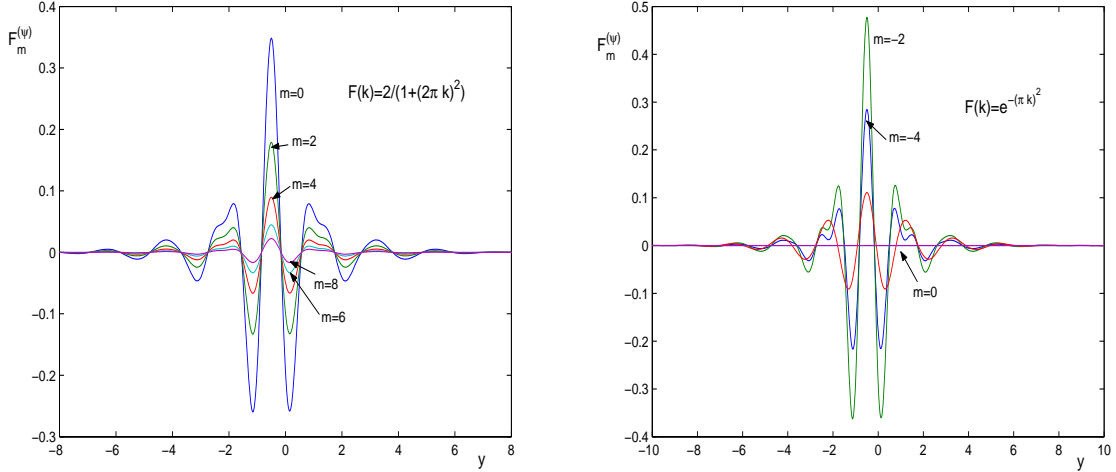


Figure 2: $\mathcal{F}_m^{(\psi)}(y)$ as a function of y , for different values of m . Left panel: $F(k) = \frac{2}{1+(2\pi k)^2}$; Right panel: $F(k) = e^{-(\pi k)^2}$.

for some $s > 0$, and the entries of the tensor Q defined by (2.3) belong to the Nikol'skii-Besov space $B_{1\infty}^\rho(\mathbb{R})$, $\rho > 1/2$. Then the following estimation is true:

$$\sup_{x \in \mathbb{R}} \sup_{r \in \mathbb{R}} \max_{i,j=1,\dots,l} |B_{ij}(r) - \langle u_i^{(FW)}(x+r) u_j^{(FW)}(x) \rangle| \leq \frac{C_s}{4^{m_1 s}} + \frac{C'_{m_0 \rho}}{b_0^{2\rho-1}(m_0)} + \sum_{m=m_0}^{m_1} \frac{C''_{m\rho}}{b_1^{2\rho-1}(m)} \quad (5.19)$$

with the relevant constants C_s , $C'_{m_0 \rho}$ and $C''_{m\rho}$ depending on F , $\hat{\phi}$, and $\hat{\psi}$.

6 Randomized models of homogeneous random fields based on plane wave decomposition

6.1 Plane wave decomposition of homogeneous random fields

Our presentation of Fourier-wavelet expansions was given above for the one-dimensional case, i.e., $\mathbf{u}(x)$, $x \in \mathbb{R}$. Direct generalizations to high-dimensional case is possible on the basis of relevant multidimensional scaling and wavelet functions, see, e.g., [45], [40]. However with the dimension, the complexity of this kind of models increases drastically. Therefore, it is reasonable to try to construct high-dimensional models via one-dimensional ones.

Here we present plane waves decomposition method for simulating random fields using samples of relevant random processes. This approach is especially efficient for isotropic random fields, see, e.g., [28], [10].

Denote by S_{d-1} a unit sphere in \mathbb{R}^d , and A_d be its surface area, $d\Omega$ the area element.

Let us introduce a function $B : \mathbb{R} \times S_{d-1} \rightarrow \mathbb{R}^{n \times n}$ such that $B(\cdot; \Omega)$ is a correlation tensor for almost all $\Omega \in S_{d-1}$. We introduce also a n -dimensional Gaussian random field

$\mathbf{Z}(t; A)$, $t \in \mathbb{R}$, and A is a measurable subset of S_{d-1} which is defined by

$$\langle \mathbf{Z}(t; A) \rangle = 0; \quad \mathbf{Z}(t; A_1 \cup A_2) = \mathbf{Z}(t; A_1) + \mathbf{Z}(t; A_2) \quad \text{for } A_1 \cap A_2 = \emptyset \quad (6.1)$$

$$\langle \mathbf{Z}(t_1; A_1) \mathbf{Z}^T(t_2; A_2) \rangle = \int_{A_1 \cap A_2} B(t_1 - t_2; \boldsymbol{\Omega}) d\boldsymbol{\Omega} \quad (6.2)$$

for each $t_1, t_2 \in \mathbb{R}$ and measurable subsets A_1, A_2, A from S_{d-1} .

The block matrix \mathcal{B} with the entries

$$B_{ij} = \int_{A_i \cap A_j} B(t_i - t_j; \boldsymbol{\Omega}), \quad i, j = 1, \dots, N \quad (6.3)$$

is positive definite and symmetric for all positive integer N and values t_1, \dots, t_N in \mathbb{R} , and measurable subsets A_1, \dots, A_N in S_{d-1} . The proof of this statement is given in Appendix A.

Thus the Gaussian random field $\mathbf{Z}(t; A)$ is well defined. Note that $\mathbf{Z}(t; \cdot)$ is a Gaussian white noise measure, for fixed t .

Let $H_i(\boldsymbol{\Omega})$, $i = 1, 2$ be complex-valued $l \times n$ -matrices depending on $\boldsymbol{\Omega} \in S_{d-1}$ satisfying the condition $\int \|H_i\|^2 d\boldsymbol{\Omega} < \infty$. We will use the following property

$$\left\langle \int_{S_{d-1}} H_1(\boldsymbol{\Omega}) \mathbf{Z}(t_1; d\boldsymbol{\Omega}) \left(\int_{S_{d-1}} H_2(\boldsymbol{\Omega}) \mathbf{Z}(t_2; d\boldsymbol{\Omega}) \right)^* \right\rangle = \int_{S_{d-1}} H_1(\boldsymbol{\Omega}) B(t_1 - t_2; \boldsymbol{\Omega}) H_2^*(\boldsymbol{\Omega}) d\boldsymbol{\Omega} . \quad (6.4)$$

Given the correlation tensor in τ , $B(\tau; \boldsymbol{\Omega})$ the spectral tensor in κ , $F_v(\kappa; \boldsymbol{\Omega})$ is defined by

$$F_v(\kappa; \boldsymbol{\Omega}) = \int_{-\infty}^{\infty} e^{-i2\pi\kappa\tau} B(\tau; \boldsymbol{\Omega}) d\tau . \quad (6.5)$$

Let $H(\boldsymbol{\Omega})$ be a $l \times n$ matrix defined on S_{d-1} . We define $\tilde{\mathbf{u}}(\mathbf{x})$ by

$$\tilde{\mathbf{u}}(\mathbf{x}) = \int_{S_{d-1}} H(\boldsymbol{\Omega}) \mathbf{Z}(\mathbf{x} \cdot \boldsymbol{\Omega}; d\boldsymbol{\Omega}) . \quad (6.6)$$

We show now that

$$\langle \tilde{\mathbf{u}}(\mathbf{x} + \mathbf{r}) \tilde{\mathbf{u}}^T(\mathbf{x}) \rangle = \int_{\mathbb{R}^d} e^{i2\pi \mathbf{r} \cdot \mathbf{k}} \frac{1}{k^{d-1}} \{ H(\hat{\mathbf{k}}) F_v(k, \hat{\mathbf{k}}) H^*(\hat{\mathbf{k}}) + H(-\hat{\mathbf{k}}) F_v(-k, -\hat{\mathbf{k}}) H^*(-\hat{\mathbf{k}}) \} d\mathbf{k} , \quad (6.7)$$

where $k = |\mathbf{k}|$, $\hat{\mathbf{k}} = \mathbf{k}/k$. This implies that the spectral tensor $\tilde{F}(\mathbf{k})$ of the random field $\tilde{\mathbf{u}}(\mathbf{x})$ is given by

$$\tilde{F}(\mathbf{k}) = \frac{1}{k^{d-1}} \{ H(\hat{\mathbf{k}}) F_v(k, \hat{\mathbf{k}}) H^*(\hat{\mathbf{k}}) + H(-\hat{\mathbf{k}}) F_v(-k, -\hat{\mathbf{k}}) H^*(-\hat{\mathbf{k}}) \} . \quad (6.8)$$

By the definition, we get from (6.4)

$$\begin{aligned}
\left\langle \tilde{\mathbf{u}}(\mathbf{x} + \mathbf{r}) \tilde{\mathbf{u}}^T(\mathbf{x}) \right\rangle &= \left\langle \int_{S_{d-1}} H(\boldsymbol{\Omega}) \mathbf{Z}((\mathbf{x} + \mathbf{r}) \cdot \boldsymbol{\Omega}; d\boldsymbol{\Omega}) \left(\int_{S_{d-1}} H(\boldsymbol{\Omega}) \mathbf{Z}(\mathbf{x} \cdot \boldsymbol{\Omega}; d\boldsymbol{\Omega}) \right)^* \right\rangle \\
&= \int_{S_{d-1}} H(\boldsymbol{\Omega}) B(\mathbf{r} \cdot \boldsymbol{\Omega}; \boldsymbol{\Omega}) H^*(\boldsymbol{\Omega}) d\boldsymbol{\Omega} = \int_{S_{d-1}} d\boldsymbol{\Omega} \int_{-\infty}^{\infty} e^{i 2\pi \boldsymbol{\kappa} \mathbf{r} \cdot \boldsymbol{\Omega}} H(\boldsymbol{\Omega}) F_v(\boldsymbol{\kappa}; \boldsymbol{\Omega}) H^*(\boldsymbol{\Omega}) d\boldsymbol{\kappa} \\
&= \int_{S_{d-1}} d\boldsymbol{\Omega} \int_0^{\infty} e^{i 2\pi \boldsymbol{\kappa} \mathbf{r} \cdot \boldsymbol{\Omega}} H(\boldsymbol{\Omega}) F_v(\boldsymbol{\kappa}; \boldsymbol{\Omega}) H^*(\boldsymbol{\Omega}) d\boldsymbol{\kappa} \\
&+ \int_{S_{d-1}} d\boldsymbol{\Omega} \int_0^{\infty} e^{-i 2\pi \boldsymbol{\kappa} \mathbf{r} \cdot \boldsymbol{\Omega}} H(\boldsymbol{\Omega}) F_v(-\boldsymbol{\kappa}; \boldsymbol{\Omega}) H^*(\boldsymbol{\Omega}) d\boldsymbol{\kappa} \\
&= \int_{S_{d-1}} d\boldsymbol{\Omega} \int_0^{\infty} e^{i 2\pi \boldsymbol{\kappa} \mathbf{r} \cdot \boldsymbol{\Omega}} \left\{ H(\boldsymbol{\Omega}) F_v(\boldsymbol{\kappa}; \boldsymbol{\Omega}) H^*(\boldsymbol{\Omega}) + H(-\boldsymbol{\Omega}) F_v(-\boldsymbol{\kappa}; -\boldsymbol{\Omega}) H^*(-\boldsymbol{\Omega}) \right\} d\boldsymbol{\kappa} \\
&= \int_{\mathbb{R}^d} e^{i 2\pi \mathbf{r} \mathbf{k}} \frac{1}{k^{d-1}} \left\{ H(\hat{\mathbf{k}}) F_v(k, \hat{\mathbf{k}}) H^*(\hat{\mathbf{k}}) + H(-\hat{\mathbf{k}}) F_v(-k, -\hat{\mathbf{k}}) H^*(-\hat{\mathbf{k}}) \right\} d\mathbf{k} . \quad (6.9)
\end{aligned}$$

Let $\mathbf{u}(\mathbf{x})$, $\mathbf{x} \in \mathbb{R}^d$ be a zero mean vector homogeneous Gaussian random field of dimension l defined by its spectral tensor $F(\mathbf{k})$. We are in position now to construct the random field $\mathbf{u}(\mathbf{x})$ as a superposition of the plane waves. Indeed, let

$$F_v(\boldsymbol{\kappa}; \boldsymbol{\Omega}) = \frac{|\boldsymbol{\kappa}|^{d-1}}{2} F(\boldsymbol{\kappa} \boldsymbol{\Omega}) , \quad H(\boldsymbol{\Omega}) = \mathbf{I} , \quad (6.10)$$

hence it follows from (6.7) that the random field

$$\mathbf{u}(\mathbf{x}) = \int_{S_{d-1}} \mathbf{Z}(\mathbf{x} \cdot \boldsymbol{\Omega}; d\boldsymbol{\Omega}) \quad (6.11)$$

has the desired spectral tensor $F(\mathbf{k})$.

Thus, we give an integral representation of homogeneous Gaussian random fields through a superposition of plane waves $\mathbf{Z}(\mathbf{x} \boldsymbol{\Omega}; d\boldsymbol{\Omega})$ (see (6.6) and (6.11)). A numerical model can be constructed through an approximation of the integral over an unit sphere by a finite sum. Here one can use both deterministic and stochastic approaches.

6.2 Decomposition with fixed nodes

Let $\Delta\boldsymbol{\Omega}_i$, $i = 1, \dots, N_s$ be a finite partition of the unit sphere S_{d-1} : $S_{d-1} = \cup_{i=1}^{N_s} \Delta\boldsymbol{\Omega}_i$, and $\Delta\boldsymbol{\Omega}_i \cap \Delta\boldsymbol{\Omega}_j = \emptyset$ when $i \neq j$. Choosing nodes $\boldsymbol{\Omega}_i \in \Delta\boldsymbol{\Omega}_i$, $i = 1, \dots, N_s$, the following deterministic approximation to (6.6) can be constructed:

$$\tilde{\mathbf{u}}(\mathbf{x}) = \int_{S_{d-1}} H(\boldsymbol{\Omega}) \mathbf{Z}(\mathbf{x} \cdot \boldsymbol{\Omega}; d\boldsymbol{\Omega}) \simeq \sum_{i=1}^{N_s} H(\boldsymbol{\Omega}_i) \mathbf{Z}(\mathbf{x} \cdot \boldsymbol{\Omega}_i; \Delta\boldsymbol{\Omega}_i), \quad (6.12)$$

where by definition (see (6.1) and (6.2)) $\mathbf{Z}(t; \Delta\Omega_i)$, $t \in \mathbb{R}$, $i = 1, \dots, N_s$ are mutually independent zero mean stationary Gaussian processes with the following correlation structure:

$$\langle \mathbf{Z}(t + \tau; \Delta\Omega_i) (\mathbf{Z}(t; \Delta\Omega_i))^T \rangle = \int_{\Delta\Omega_i} B(\tau; \Omega) d\Omega = \int_{\Delta\Omega_i} \int_{-\infty}^{\infty} e^{i2\pi \kappa \tau} F_v(\kappa; \Omega) d\kappa d\Omega.$$

From this it follows that the process $\mathbf{Z}(t; \Delta\Omega_i)$, $t \in \mathbb{R}$ has a spectral tensor given by $\int_{\Delta\Omega_i} F_v(\kappa; \Omega) d\Omega \simeq |\Delta\Omega_i| F_v(\kappa; \Omega_i)$, where $|\Delta\Omega_i| = \int_{\Delta\Omega_i} d\Omega$. therefore, the process $\mathbf{Z}(t; \Delta\Omega_i)$ can be approximated by $|\Delta\Omega_i|^{1/2} \mathbf{v}^{(i)}(t)$ where $\mathbf{v}^{(i)}(t) = (v_1^{(i)}(t), \dots, v_n^{(i)}(t))^T$ is a random process with the spectral tensor $F_v(\kappa; \Omega_i)$. From this we get by (6.12) the following approximation to the random field $\tilde{\mathbf{u}}(\mathbf{x})$, $\mathbf{x} \in \mathbb{R}^d$:

$$\tilde{\mathbf{u}}_{N_s}^{det}(\mathbf{x}) = \sum_{i=1}^{N_s} |\Delta\Omega_i|^{1/2} H(\Omega_i) \mathbf{v}^{(i)}(\mathbf{x} \cdot \Omega_i) \quad (6.13)$$

By the construction it is clear that the smaller the subregions $\Delta\Omega_i$, $i = 1, \dots, N_s$ the better $\tilde{\mathbf{u}}_{N_s}^{det}(\mathbf{x})$ approximates the random field with the spectral tensor (6.8). In particular the model

$$\mathbf{u}_{N_s}^{det}(\mathbf{x}) = \sum_{i=1}^{N_s} |\Delta\Omega_i|^{1/2} \mathbf{v}^{(i)}(\mathbf{x} \cdot \Omega_i) \quad (6.14)$$

where $\mathbf{v}^{(i)}(t) = (v_1^{(i)}(t), \dots, v_l^{(i)}(t))^T$, $i = 1, \dots, N_s$ are mutually independent zero mean Gaussian processes with spectral tensor $F^{(i)}(\kappa) = \frac{|\kappa|^{d-1}}{2} F(\kappa \Omega_i)$ is an approximation of the random field $\mathbf{u}(\mathbf{x}) = (u_1(\mathbf{x}), \dots, u_l(\mathbf{x}))^T$, $\mathbf{x} \in \mathbb{R}^d$ having spectral tensor $F(\mathbf{k})$.

Let us consider the case when the spectral tensor $F(\mathbf{k})$ has the form

$$F(\mathbf{k}) = H(\hat{\mathbf{k}}) H^*(\hat{\mathbf{k}}) \frac{2E(k)}{A_d k^{d-1}}, \quad (6.15)$$

where $H(\Omega)$, $\Omega \in S_{d-1}$ is an $l \times n$ -matrix satisfying the condition

$$H(-\Omega) H^*(-\Omega) = H(\Omega) H^*(\Omega), \quad (6.16)$$

and $E(k)$ is a scalar non-negative even function, A_d is the area of the unit sphere in \mathbb{R}^d .

Thus the approximation to the random field $\mathbf{u}(\mathbf{x}) = (u_1(\mathbf{x}), \dots, u_l(\mathbf{x}))^T$, $\mathbf{x} \in \mathbb{R}^d$ with the spectrum (6.15) can be constructed by the formula:

$$\mathbf{u}_{N_s}^{det}(\mathbf{x}) = \sum_{i=1}^{N_s} \left(\frac{|\Delta\Omega_i|}{A_d} \right)^{1/2} H(\Omega_i) \mathbf{v}^{(i)}(\mathbf{x} \cdot \Omega_i) \quad (6.17)$$

where $\mathbf{v}^{(i)}(t) = (v_1^{(i)}(t), \dots, v_n^{(i)}(t))^T$, $i = 1, \dots, N_s$ are mutually independent zero mean, stationary, Gaussian random processes with independent components each having the same spectral function $F_v(\kappa) = E(\kappa)$:

$$\langle v_{j_1}^{(i_1)}(t + \tau) v_{j_2}^{(i_2)}(t) \rangle = \delta_{i_1 i_2} \delta_{j_1 j_2} \int_{-\infty}^{\infty} e^{i2\pi \kappa \tau} E(\kappa) d\kappa.$$

A homogeneous d -dimensional vector random field $\mathbf{u}(x)$, $\mathbf{x} \in \mathbb{R}^d$ is called isotropic if the random field $\mathbf{v}(\mathbf{x}) = U^T \mathbf{u}(U\mathbf{x})$ has the same finite-dimensional distributions as those of the random field $\mathbf{u}(\mathbf{x})$ for any rotation U with transpose U^T (e.g., see [32]). It is known that the general structure of the spectral tensor of an isotropic random field is the following [32]:

$$F_{ij}(\mathbf{k}) = \frac{2}{A_d k^{d-1}} \left\{ E_1(k) \left(\delta_{ij} - \frac{k_i k_j}{k^2} \right) + E_2(k) \frac{k_i k_j}{k^2} \right\} \quad (6.18)$$

where $k = |\mathbf{k}|$, A_d is the area of the unit sphere in \mathbb{R}^d , E_1 and E_2 are non-negative scalar even functions.

The tensor (6.18) can be represented in the form

$$F(\mathbf{k}) = \frac{2E_1(k)}{A_d k^{d-1}} H_1(\hat{\mathbf{k}}) H_1^*(\hat{\mathbf{k}}) + \frac{2E_2(k)}{A_d k^{d-1}} H_2(\hat{\mathbf{k}}) H_2^*(\hat{\mathbf{k}}) \quad (6.19)$$

where $H_1 = (h_{ij}^{(1)})_{i,j=1}^d$ and $H_2 = (h_1^{(2)}, \dots, h_d^{(2)})$ are $d \times d$ and $1 \times d$ matrix functions defined on the unit sphere S_{d-1} by

$$h_{ij}^{(1)}(\boldsymbol{\Omega}) = \delta_{ij} - \Omega_i \Omega_j; \quad h_j^{(2)}(\boldsymbol{\Omega}) = \Omega_j, \quad i, j = 1, \dots, d, \quad \boldsymbol{\Omega} = (\Omega_1, \dots, \Omega_d) \in S_{d-1}.$$

The tensors H_i , $i = 1, 2$ obviously satisfy (6.16). Therefore, the random field $\mathbf{u}(\mathbf{x})$ can be approximated by

$$\mathbf{u}_{N_s}^{det}(\mathbf{x}) = \sum_{i=1}^{N_s} \left(\frac{|\Delta \boldsymbol{\Omega}_i|}{A_d} \right)^{1/2} \left(H_1(\boldsymbol{\Omega}_i) \mathbf{v}_1^{(i)}(\mathbf{x} \cdot \boldsymbol{\Omega}_i) + H_2(\boldsymbol{\Omega}_i) \mathbf{v}_2^{(i)}(\mathbf{x} \cdot \boldsymbol{\Omega}_i) \right) \quad (6.20)$$

where $\mathbf{v}_1^{(i)}$, and $\mathbf{v}_2^{(i)}$ $i = 1, \dots, N_s$ are mutually independent zero mean, stationary d -dimensional, Gaussian random processes with independent components. Each component of $\mathbf{v}_1^{(i)}(t)$ has the spectral function $E_1(\kappa)$, and each component of $\mathbf{v}_2^{(i)}(t)$ has the spectral function $E_2(\kappa)$. Let $v^{(i)}(t) = H_2(\boldsymbol{\Omega}_i) \mathbf{v}_2^{(i)}(t) = \boldsymbol{\Omega}_i \cdot \mathbf{v}_2^{(i)}(t)$. It is not difficult to check that the spectral function of the scalar process $v^{(i)}(t)$, $t \in \mathbb{R}$ is $E_2(\kappa)$. Thus we can present the formula (6.20) in a form convenient for simulation

$$\mathbf{u}_{N_s}^{det}(\mathbf{x}) = \sum_{i=1}^{N_s} \left(\frac{|\Delta \boldsymbol{\Omega}_i|}{A_d} \right)^{1/2} \left(H_1(\boldsymbol{\Omega}_i) \mathbf{v}_1^{(i)}(\mathbf{x} \cdot \boldsymbol{\Omega}_i) + v^{(i)}(\mathbf{x} \cdot \boldsymbol{\Omega}_i) \right) \quad (6.21)$$

where $v^{(i)}(t)$, $i = 1, \dots, N_s$ is a set of independent of each other and on $\mathbf{v}_1^{(i)}(t)$, $i = 1, \dots, N_s$ scalar random processes with the spectral function $E_2(\kappa)$.

6.3 Decomposition with randomly distributed nodes

A randomized model of the field $\tilde{\mathbf{u}}(\mathbf{x})$, $\mathbf{x} \in \mathbb{R}^d$ defined by the stochastic integral (6.6) with the spectral tensor (6.8) can be represented in the form:

$$\tilde{\mathbf{u}}_{N_s}^{rnd}(\mathbf{x}) = \frac{A_d^{1/2}}{N_s^{1/2}} \sum_{i=1}^{N_s} H(\boldsymbol{\omega}_i) \mathbf{v}^{(i)}(\mathbf{x} \cdot \boldsymbol{\omega}_i), \quad (6.22)$$

where $\boldsymbol{\omega}_i, i = 1, \dots, N_s$ is a family of independent unit isotropic vectors in \mathbb{R}^d , $\mathbf{v}^{(i)}(t) = (v_1^{(i)}(t), \dots, v_n^{(i)}(t))^T$, $i = 1, \dots, N_s$ is a set of mutually independent and stochastically independent of $\boldsymbol{\omega}_i, i = 1, \dots, N_s$, zero mean, stationary Gaussian random processes with the spectral tensor $F_v(\kappa, \boldsymbol{\omega}_i)$.

In general case of anisotropic random fields, the following generalization of the model (6.22) can be given

$$\tilde{\mathbf{u}}_{N_s}^{rnd}(\mathbf{x}) = \frac{1}{N_s^{1/2}} \sum_{i=1}^{N_s} \frac{1}{p^{1/2}(\boldsymbol{\omega}_i)} H(\boldsymbol{\omega}_i) \mathbf{v}^{(i)}(\mathbf{x} \cdot \boldsymbol{\omega}_i), \quad (6.23)$$

where $p(\boldsymbol{\Omega})$, $\boldsymbol{\Omega} \in S_{d-1}$ is a probability density function defined on a unit sphere S_{d-1} , and the random points $\boldsymbol{\omega}_i, i = 1, \dots, N_s$ are independently sampled on S_{d-1} according to the density $p(\boldsymbol{\Omega})$; the family $\mathbf{v}^{(i)}(t)$ is constructed the same as in (6.22).

Proposition 3. Suppose that the density $p(\boldsymbol{\Omega})$ satisfies the condition

$$p(\boldsymbol{\Omega}) > 0 \quad \text{if} \quad \int_{-\infty}^{\infty} F_v(\kappa; \boldsymbol{\Omega}) d\kappa > 0. \quad (6.24)$$

Then for any N_s the function $\tilde{\mathbf{u}}_{N_s}^{rnd}(\mathbf{x})$ defined by (6.23) is a zero mean homogeneous random field (generally non-Gaussian) with the spectral tensor (6.8):

$$\langle \tilde{\mathbf{u}}_{N_s}^{rnd}(\mathbf{x} + \mathbf{r}) (\tilde{\mathbf{u}}_{N_s}^{rnd}(\mathbf{x}))^T \rangle = \int_{\mathbb{R}^d} e^{i2\pi \mathbf{r} \cdot \mathbf{k}} \tilde{F}(\mathbf{k}) d\mathbf{k}. \quad (6.25)$$

Proof. The terms in the sum of (6.23) are independent; also, the process $\mathbf{v}^{(i)}(t)$ is independent of $\boldsymbol{\omega}_i$, hence,

$$\langle \tilde{\mathbf{u}}_{N_s}^{rnd}(\mathbf{x} + \mathbf{r}) (\tilde{\mathbf{u}}_{N_s}^{rnd}(\mathbf{x}))^T \rangle = \langle \tilde{\mathbf{u}}_1^{rnd}(\mathbf{x} + \mathbf{r}) (\tilde{\mathbf{u}}_1^{rnd}(\mathbf{x}))^T \rangle = \langle H(\boldsymbol{\omega}) \langle \mathbf{v}_{\boldsymbol{\omega}}((\mathbf{x} + \mathbf{r})\boldsymbol{\omega}) \mathbf{v}_{\boldsymbol{\omega}}^T(\mathbf{x}\boldsymbol{\omega}) | \boldsymbol{\omega} \rangle H^*(\boldsymbol{\omega}) \rangle,$$

where $\boldsymbol{\omega}$ is a random point in S_{d-1} having the density $p(\boldsymbol{\Omega})$; The random process $\mathbf{v}_{\boldsymbol{\omega}}(t)$ is stochastically independent of $\boldsymbol{\omega}$, having a spectral tensor $F_v(\kappa; \boldsymbol{\omega})$; Here $\langle \cdot | \boldsymbol{\omega} \rangle$ means a conditional avergaing under a fixed $\boldsymbol{\omega}$. By the construction,

$$\langle \mathbf{v}_{\boldsymbol{\omega}}((\mathbf{x} + \mathbf{r})\boldsymbol{\omega}) \mathbf{v}_{\boldsymbol{\omega}}^T(\mathbf{x}\boldsymbol{\omega}) | \boldsymbol{\omega} \rangle = \int_{-\infty}^{\infty} e^{i2\pi \kappa \mathbf{r} \cdot \boldsymbol{\omega}} F_v(\kappa; \boldsymbol{\omega}) d\kappa.$$

Therefore,

$$\langle H(\boldsymbol{\omega}) \langle \mathbf{v}_{\boldsymbol{\omega}}((\mathbf{x} + \mathbf{r})\boldsymbol{\omega}) \mathbf{v}_{\boldsymbol{\omega}}^T(\mathbf{x}\boldsymbol{\omega}) | \boldsymbol{\omega} \rangle H^*(\boldsymbol{\omega}) \rangle = \int_{S_{d-1}} d\boldsymbol{\Omega} \int_{-\infty}^{\infty} e^{i2\pi \kappa \mathbf{r} \cdot \boldsymbol{\Omega}} H(\boldsymbol{\Omega}) F_v(\kappa; \boldsymbol{\Omega}) H^*(\boldsymbol{\Omega}) d\kappa.$$

Then we can proceed as we have done after the second row in (6.9); this leads us to the desired relation (6.25).

Assume that the spectral tensor of the random field to be simulated has a representation (6.15) where the tensor H satisfies (6.16). Then, it is reasonable to choose $p(\boldsymbol{\Omega}) \equiv 1/A_d$,

which means the points on $\boldsymbol{\omega}_i$ are distributed uniformly; thus the simulation formula can be written as follows

$$\mathbf{u}_{N_s}^{rnd}(\mathbf{x}) = \frac{1}{N_s^{1/2}} \sum_{i=1}^{N_s} H(\boldsymbol{\omega}_i) \mathbf{v}^{(i)}(\mathbf{x} \cdot \boldsymbol{\omega}_i) \quad (6.26)$$

where $\mathbf{v}^{(i)}(t) = (v_1^{(i)}(t), \dots, v_m^{(i)}(t))^T$, $i = 1, \dots, N_s$ are mutually independent zero mean stationary Gaussian random processes with independent components having the same spectral function $E(\kappa)$. A d -dimensional isotropic random field with a spectral density (6.18) is simulated by

$$\mathbf{u}_{N_s}^{rnd}(\mathbf{x}) = \frac{1}{N_s^{1/2}} \sum_{i=1}^{N_s} \left(H_1(\boldsymbol{\omega}_i) \mathbf{v}_1^{(i)}(\mathbf{x} \cdot \boldsymbol{\omega}_i) + v^{(i)}(\mathbf{x} \cdot \boldsymbol{\omega}_i) \right) \quad (6.27)$$

where $\boldsymbol{\omega}_i$, $i = 1, \dots, N_s$ is a family of independent unit isotropic vectors in \mathbb{R}^d ; $\mathbf{v}_1^{(i)}$ and $v^{(i)}$ $i = 1, \dots, N_s$ are mutually independent and stochastically independent of $\boldsymbol{\omega}_i$, $i = 1, \dots, N_s$, zero mean, stationary d -dimensional scalar Gaussian random processes with independent components. Components of $\mathbf{v}_1^{(i)}(t)$ are independent of each other and have the same spectral function $E_1(\kappa)$ while the random process $v^{(i)}(t)$ has the spectral function $E_2(\kappa)$. Note that the representation (6.27) is given in [28].

6.4 Decomposition with stratified randomly distributed nodes

It is possible to construct a stratified randomization model by choosing a subdivision $\{\Delta\Omega_i\}_{i=1}^{N_s}$ and then in each $\Delta\Omega_i$ a random point $\boldsymbol{\omega}_i \in \Delta\Omega_i$ is sampled; for simplicity, we may assume that it is uniformly distributed in $\Delta\Omega_i$. So under the condition (6.15) we can use, along with the models (6.17) and (6.26) the following model with stratified randomly distributed nodes:

$$\mathbf{u}_{N_s}^{srm}(\mathbf{x}) = \sum_{i=1}^{N_s} \left(\frac{|\Delta\Omega_i|}{A_d} \right)^{1/2} H(\boldsymbol{\omega}_i) \mathbf{v}^{(i)}(\mathbf{x} \cdot \boldsymbol{\omega}_i) \quad (6.28)$$

7 Comparison of Fourier wavelet and randomized spectral models

As mentioned in the Introduction, our experiments in one-dimensional case ($d = 1$) have shown that the randomized models are more efficient in evaluation of ensemble averages than the FW models, or compatible in efficiencies, if mult-point statistics should be calculated, see [23]. The situation is opposite for a spatial averaging.

In this section we compare the Fourier-Wavelet Model (FWM) and the Randomized Spectral Model (RSM) in the three-dimensional case ($d = 3$). We simulate a three-dimensional zero mean Gaussian isotropic incompressible random field $\mathbf{u}(\mathbf{x})$ with a spectral tensor

$$F_{ij}(\mathbf{k}) = \frac{2E(k)}{4\pi k^2} \left(\delta_{ij} - \frac{k_i k_j}{k^2} \right), \quad i, j = 1, 2, 3; \quad E(k) = \frac{8(2\pi k)^4}{(1 + (2\pi k)^2)^3}. \quad (7.1)$$

It is known that the correlation tensor of isotropic incompressible fields is defined by $B_{LL}(r)$, the longitudinal, and $B_{NN}(r)$, transversal correlation functions, e.g., see [32]. In our case these functions can be represented explicitly (e.g., see [32]):

$$\begin{aligned} B_{LL}(r) &= \langle u_1(x+r, 0, 0)u_1(x, 0, 0) \rangle = e^{-r}, \\ B_{NN}(r) &= \langle u_2(x+r, 0, 0)u_2(x, 0, 0) \rangle = e^{-r}(1-r/2). \end{aligned} \quad (7.2)$$

The comparison of RSM and FWM is made by calculations of Eulerian and Lagrangian stochastic characteristics of the random field $\mathbf{u}(\mathbf{x})$ with the spectral tensor (7.1). The Eulerian characteristics are namely the correlation functions (7.2). The Lagrangian characteristics are the Lagrangian correlation function $B_{ij}^{(L)}(t) = \langle V_i(t)V_j(0) \rangle$ and the diffusion coefficient $K_L(t) = \frac{1}{6} \frac{d}{dt} \langle (\mathbf{X}(t) - \mathbf{x}_0)^2 \rangle$, where $\mathbf{V}(t) = (V_1(t), V_2(t), V_3(t)) = \frac{d\mathbf{X}(t)}{dt}$ is the Lagrangian velocity, and $\mathbf{X}(t) = (X_1(t), X_2(t), X_3(t))$ is the Lagrangian trajectory starting at the point \mathbf{x}_0 :

$$\frac{d\mathbf{X}(t)}{dt} = \mathbf{u}(\mathbf{X}(t)), \quad \mathbf{X}(0) = \mathbf{x}_0. \quad (7.3)$$

7.1 Some technical details of RSM.

As a basis, we take the model (4.5) for the simulation of isotropic random field $\mathbf{u}(\mathbf{x})$. The spectral space is divided in $N = 3$ subsets $\Delta_i = \{\mathbf{k} : a_i \leq |\mathbf{k}| < b_i\}$, $i = 1, 2, 3$ with $a_1 = 0$, $b_1 = a_2 = 0.34$, $b_2 = a_3 = 0.8$, $b_3 = \infty$. In each subset Δ_i n_0 points $\mathbf{k}_{i,j}$, $j = 1, \dots, n_0$ are sampled with the same probability density

$$p_i(\mathbf{k}) = \frac{1}{4\pi k^2} \frac{C_i}{(1 + (2\pi k)^2)}, \quad \mathbf{k} \in \Delta_i; \quad C_i = 1 / \int_{a_i}^{b_i} \frac{dk}{(1 + (2\pi k)^2)}.$$

Note that the spectral tensor (7.1) can be written in the form (2.3) with $Q(\mathbf{k}) = f^{1/2}(\mathbf{k})H(\hat{\mathbf{k}})$:

$$F(\mathbf{k}) = f^{1/2}(\mathbf{k})H(\hat{\mathbf{k}}) \left(f^{1/2}(\mathbf{k})H(\hat{\mathbf{k}}) \right)^T; \quad f(\mathbf{k}) = 16\pi \frac{(2\pi k)^2}{(1 + (2\pi k)^2)^3},$$

and the entries $h_{ij}(\boldsymbol{\Omega})$ of 3×3 -dimensional antisymmetric matrix $H(\boldsymbol{\Omega})$, $\boldsymbol{\Omega} \in S_2$ are defined by

$$\begin{aligned} h_{ii}(\boldsymbol{\Omega}) &= 0, \quad i = 1, 2, 3; \quad h_{12}(\boldsymbol{\Omega}) = -h_{21}(\boldsymbol{\Omega}) = \Omega_3; \quad h_{13}(\boldsymbol{\Omega}) = -h_{31}(\boldsymbol{\Omega}) = -\Omega_2; \\ & \quad h_{23}(\boldsymbol{\Omega}) = -h_{32}(\boldsymbol{\Omega}) = \Omega_1. \end{aligned}$$

For a 3-dimensional vector $\boldsymbol{\xi} = H(\hat{\mathbf{k}})\boldsymbol{\xi} = \hat{\mathbf{k}} \times \boldsymbol{\xi}$ ($\mathbf{a} \times \mathbf{b}$ is a vector product of vectors \mathbf{a} and \mathbf{b}), hence in view of (4.5) we come to the simulation formula

$$\mathbf{u}_{N,n_0}(\mathbf{x}) = \sum_{i=1}^N \frac{1}{\sqrt{n_0}} \sum_{j=1}^{n_0} \left(\frac{f(\mathbf{k}_{ij})}{p_i(\mathbf{k}_{ij})} \right)^{1/2} \{ (\boldsymbol{\omega}_{ij} \times \boldsymbol{\xi}_{ij}) \cos(\theta_{ij}) + (\boldsymbol{\omega}_{ij} \times \boldsymbol{\eta}_{ij}) \sin(\theta_{ij}) \} \quad (7.4)$$

where $\mathbf{k}_{ij} = k_{ij}\boldsymbol{\omega}_{ij}$, $\boldsymbol{\omega}_{ij}$, $i = 1, \dots, N$; $j = 1, \dots, n_0$ are mutually independent 3-dimensional unit isotropic vectors, and k_{ij} $i = 1, \dots, N$; $j = 1, \dots, n_0$ are random

points (independent of each other and of $\boldsymbol{\omega}_{ij}$) distributed in $[a_i, b_i]$ with the density $p_i(k) = C_i/(1 + (2\pi k)^2)$. Here $\theta_{ij} = 2\pi k_{ij} \boldsymbol{\omega}_{ij} \cdot \mathbf{x}$, and $\boldsymbol{\xi}_{ij}, \boldsymbol{\eta}_{ij}, i = 1, \dots, N; j = 1, \dots, n_\theta$ are mutually independent and independent of the family \mathbf{k}_{ij} standard 3-dimensional Gaussian random variables (with zero mean and unity covariance matrix).

The points \mathbf{k}_{ij} in (7.4) are sampled isotropically which does not imply that the samples of $\mathbf{u}_{N, n_\theta}(\mathbf{x})$ are isotropic in space, especially when n_θ are relatively small. To improve the isotropic property, it is reasonable to apply a stratified sampling over angles. So to choose a subdivision of the unite sphere in \mathbb{R}^3 , we work in the spherical coordinates $(\theta, \phi), 0 \leq \theta \leq \pi, 0 \leq \phi \leq 2\pi$. First we fix an integer parameter $n_\theta \geq 1$ which defines the step $\Delta\theta = \pi/n_\theta$ and the relevant altitude mesh $\theta_j = (j - 1/2)\Delta\theta, j = 1, \dots, n_\theta$. For each fixed $j, (1 \leq j \leq n_\theta)$, we construct the latitude mesh $\phi_{jr} = (r - 1/2)\Delta\phi_j, r = 1, \dots, n_\phi^{(j)}$, where $n_\phi^{(j)} = \lfloor 2\pi \sin(\theta_j)/\Delta\theta \rfloor, \Delta\phi_j = 2\pi/n_\phi^{(j)}$. Finally, a two-index subdivision $\{\{\Delta\Omega_{j,r}\}_{r=1}^{n_\phi^{(j)}}, j = 1, \dots, n_\theta\}$ of the unit sphere S_2 :

$$\Delta\Omega_{j,r} = \left\{ (\theta, \phi) : \theta_j - \frac{\Delta\theta}{2} \leq \theta < \theta_j + \frac{\Delta\theta}{2}; \quad \phi_{jr} - \frac{\Delta\phi_j}{2} \leq \phi < \phi_{jr} + \frac{\Delta\phi_j}{2} \right\}, \quad (7.5)$$

is constructed, which consists of $N_s = N_s(n_\theta) = \sum_{j=1}^{n_\theta} n_\phi^{(j)}$ surface elements.

Thus we constructed the subdivision of the space $\mathbb{R}^3 = \sum_{i,j,r} \Delta_{ijr}$, where

$$\Delta_{ijr} = \{\mathbf{k} \in \mathbb{R}^3 : a_i \leq |\mathbf{k}| < b_i; \hat{\mathbf{k}} = \mathbf{k}/|\mathbf{k}| \in \Delta\Omega_{j,r}\},$$

where $i = 1, \dots, N; j = 1, \dots, n_\theta; r = 1, \dots, n_\phi^{(j)}$. In each element Δ_{ijr} we sample one point $\mathbf{k}_{ijr} = k_{ijr} \boldsymbol{\omega}_{ijr}$, where k_{ijr} is chosen in $[a_i, b_i)$ with the density $p_i(k) = C_i/(1 + (2\pi k)^2)$, while the random direction $\boldsymbol{\omega}_{ijr}$ is sampled uniformly in $\Delta\Omega_{j,r}$:

$$\boldsymbol{\omega}_{ijr} = (\sin(\tilde{\theta}_{ij}) \cos(\tilde{\phi}_{ijr}), \sin(\tilde{\theta}_{ij}) \sin(\tilde{\phi}_{ijr}), \cos(\tilde{\theta}_{ij}))$$

where $\tilde{\theta}_{ij} = \arccos((1 - \gamma_{ij}) \cos(\theta_j - \Delta\theta/2) + \gamma_{ij} \cos(\theta_j + \Delta\theta/2)), \tilde{\phi}_{ijr} = \phi_{jr} + (\gamma_{ijr} - 1/2)\Delta\phi_j$. Here $\gamma_{ij}, \gamma_{ijr} (i = 1, \dots, N; j = 1, \dots, n_\theta; r = 1, \dots, n_\phi^{(j)})$ are mutually independent random numbers uniformly distributed in $[0, 1]$. The random point \mathbf{k}_{ijr} is distributed with the density

$$p_{ijk}(\mathbf{k}) = \frac{1}{|\Delta\Omega_{j,r}|} \frac{C_i}{|\mathbf{k}|^2(1 + (2\pi|\mathbf{k}|)^2)}.$$

Thus the RSM for an isotropic Gaussian incompressible random field with the spectral tensor (7.1) constructed from the described expansion has the form:

$$\mathbf{u}_{N, n_\theta}(\mathbf{x}) = \sum_{i=1}^N \sum_{j=1}^{n_\theta} \sum_{r=1}^{n_\phi^{(j)}} \left(\frac{f(\mathbf{k}_{ijr})}{p_{ijk}(\mathbf{k}_{ijr})} \right)^{1/2} \{ (\boldsymbol{\omega}_{ijr} \times \boldsymbol{\xi}_{ijr}) \cos(\theta_{ijr}) + (\boldsymbol{\omega}_{ijr} \times \boldsymbol{\eta}_{ijr}) \sin(\theta_{ijr}) \} \quad (7.6)$$

where $\theta_{ijr} = 2\pi k_{ijr} \boldsymbol{\omega}_{ijr} \cdot \mathbf{x}$, and $\boldsymbol{\xi}_{ijr}, \boldsymbol{\eta}_{ijr}, i = 1, \dots, N; j = 1, \dots, n_\theta; r = 1, \dots, n_\phi^{(j)}$ are mutually independent and independent of the family \mathbf{k}_{ijr} standard 3-dimensional Gaussian random variables (with zero mean and unity covariance matrix).

7.2 Some technical details of FWM

Simulation formula for a 3–dimensional isotropic incompressible random field $\mathbf{u}(\mathbf{x})$ with the spectral tensor (7.1) is constructed through the plane wave decomposition, without a stratification, using the model (6.26), or with stratification, on the basis of (6.17) and (6.28), where the random processes $\mathbf{v}^{(i)}(t)$, $i = 1, \dots, N_s$ are constructed by FWM (5.10). In our case, the 3D FWM based on plane wave decomposition without a stratification has the form

$$\mathbf{u}_{N_s}^{rnd}(\mathbf{x}) = \frac{1}{N_s^{1/2}} \sum_{i=1}^{N_s} \boldsymbol{\omega}_i \times \mathbf{v}^{(i)}(\boldsymbol{\omega}_i \cdot \mathbf{x}), \quad (7.7)$$

where $\boldsymbol{\omega}_i$, $i = 1, \dots, N_s$ are mutually independent 3–dimensional unit isotropic vectors, and $\mathbf{v}^{(i)}(t)$, $i = 1, \dots, N_s$ are mutually independent 3–dimensional stationary Gaussian processes with independent identically distributed components. Each component of the process $\mathbf{v}^{(i)}(t)$ has the spectral function $F(k) = E(k)$

In the case of stratified models, the subdivision of the unit sphere appeared in (6.17) and (6.28) is constructed as described in the previous section.

Thus the 3D FWM based on the plane wave decomposition with deterministic nodes (i.e., with (6.17)) is

$$\mathbf{u}_{n_\theta}^{det}(\mathbf{x}) = \sum_{j=1}^{n_\theta} \sum_{r=1}^{n_\phi^{(j)}} \left(\frac{|\Delta\boldsymbol{\Omega}_{j,r}|}{4\pi} \right)^{1/2} \boldsymbol{\Omega}_{j,r} \times \mathbf{v}^{(jr)}(\mathbf{x} \cdot \boldsymbol{\Omega}_{j,r}), \quad (7.8)$$

where

$$\begin{aligned} \boldsymbol{\Omega}_{j,r} &= (\sin(\theta_j) \cos(\phi_{jr}), \sin(\theta_j) \sin(\phi_{jr}), \cos(\theta_j)), \\ |\Delta\boldsymbol{\Omega}_{j,r}| &= \int_{\Delta\boldsymbol{\Omega}_{j,r}} d\boldsymbol{\Omega} = 4\pi \Delta\phi_j [\cos(\theta_j - \Delta\theta/2) - \cos(\theta_j + \Delta\theta/2)]. \end{aligned}$$

A hybrid stratified randomized FWM based on the plane wave decomposition (6.28) has the form

$$\mathbf{u}_{n_\theta}^{strm}(\mathbf{x}) = \sum_{j=1}^{n_\theta} \sum_{r=1}^{n_\phi^{(j)}} \left(\frac{|\Delta\boldsymbol{\Omega}_{j,r}|}{4\pi} \right)^{1/2} \boldsymbol{\omega}_{j,r} \times \mathbf{v}^{(jr)}(\mathbf{x} \cdot \boldsymbol{\omega}_{j,r}), \quad (7.9)$$

where

$$\boldsymbol{\omega}_{jr} = (\sin(\tilde{\theta}_j) \cos(\tilde{\phi}_{jr}), \sin(\tilde{\theta}_j) \sin(\tilde{\phi}_{jr}), \cos(\tilde{\theta}_j)),$$

$$\tilde{\theta}_j = \arccos((1 - \gamma_j) \cos(\theta_j - \Delta\theta/2) + \gamma_j \cos(\theta_j + \Delta\theta/2)), \quad \tilde{\phi}_{jr} = \phi_{jr} + (\gamma_{jr} - 1/2)\Delta\phi_j,$$

and γ_j , γ_{jr} , ($j = 1, \dots, n_\theta$; $r = 1, \dots, n_\phi^{(j)}$) are mutually independent random numbers uniformly distributed on $[0, 1]$. The stationary random processes $\mathbf{v}^{(jr)}(t)$ ($j = 1, \dots, n_\theta$; $r = 1, \dots, n_\phi^{(j)}$), appeared in (7.8) and (7.9) are mutually independent 3–dimensional stationary Gaussian processes with independent identically distributed components. Each component of the process $\mathbf{v}^{(jr)}(t)$ has the spectral function $F(k) = E(k)$ (see (7.1)) and is simulated by FWM (5.10). Since all three components of all these random processes have the same spectral function, in the simulation formulae one and the same set of functions $\mathcal{F}_{m_0}^{(\phi)}$ and $\mathcal{F}_m^{(\psi)}$, $m = m_0, \dots, m_1$ is used.

Parameters of the Fourier wavelet model (5.10) are taken as $b_0 = b_1 = 10; m_0 = 0, m_1 = 6$.

Now let us give some details related to the simulation of random fields (7.7) - (7.9). So assume we have to simulate the random field $\mathbf{u}_{n_\theta}^{det}(\mathbf{x})$ (or $\mathbf{u}_{n_\theta}^{srm}(\mathbf{x})$) in a bounded domain $D \subset \mathbb{R}^3$. We choose segments $[a_{jr}, b_{jr}]$ ($j = 1, \dots, n_\theta; r = 1, \dots, n_\phi^{(j)}$) so that $\mathbf{x} \cdot \boldsymbol{\Omega}_{j,r} \in [a_{jr}, b_{jr}] \forall \mathbf{x} \in D$. Then we simulate by the FW model (5.10) the processes $\mathbf{v}^{(jr)}(t)$, $j = 1, \dots, n_\theta; r = 1, \dots, n_\phi^{(j)}$ on a sufficiently fine grid on $[a_{jr}, b_{jr}]$. The quantities $\mathbf{v}^{(ij)}(\mathbf{x} \cdot \boldsymbol{\Omega}_{i,j})$ are evaluated through a linear interpolation of the values $\mathbf{v}^{(ij)}$ obtained on this fine grid. The same can be done for the model (7.7).

The Eulerian and Lagrangean statistical characteristics ($B_{LL}(r)$, $B_{NN}(r)$, $B^{(L)}(t)$ and $K_L(t)$) defined above are calculated through ensemble and spatial averaging, by FWM and RSM.

7.3 Ensemble averaging

In Figure 3 we plot the functions $B_{LL}(r)$ and $B_{NN}(r)$ for a Gaussian isotropic incompressible random field with the spectral tensor (7.1). In Figure 4 the relevant Lagrangian correlation function $B^L(t) = B_{ii}^L(t)/3$ (left panel) and the diffusion coefficient $K_L(t)$ (right panel) are shown. The calculations are obtained by RSM (7.4) (left panels) and FWM (7.7) (right panels). The number of MC samples here and in all ensemble averagings was taken as 16000.

It is seen that with the chosen parameters, both models give very accurate plots which are practically lying on the explicit curves.

We studied numerically how the error of the model (7.4) depends on the parameter n_0 , and also, the dependence of the error of the model (7.7) on N_s . In Figure 5 we show the relevant results for $B_{LL}(r)$ and $B_{NN}(r)$, for different values of n_0 in the model (7.4). It is seen (left panel) that with $n_0 = 3$ the results are not achieved the accuracy obtained with $n_0 = 25$. On the other hand, increasing n_0 from 25 to 50 does not change the results. The same is true for the results obtained by the model (7.7) (see Figure 6).

The models (7.6) and (7.9) show a similar behaviour: already with $n_\theta = 4$ (the number of terms in (7.6) and (7.9) is $N_s = 20$) this two models give practically the same results.

The situation with the model (7.8) is different. To get a numerically stable result (to within 0.02 of absolute error) we have to take n_θ not less than 10 (the number of terms $N_s = 124$). This is because for small values of n_θ , the subdivision (7.5) of the unit sphere S_2 is crude. This is illustrated by the results presented in Figure 7 and Table 2. The quantities ϵ_{LL} and ϵ_{NN} are defined as

$$\epsilon_{LL} = \sup_{0 \leq r \leq 5} |B_{LL}^{(th)}(r) - e^{-r}|, \quad \epsilon_{NN} = \sup_{0 \leq r \leq 5} |B_{NN}^{(th)}(r) - e^{-r}(1 - r/2)|,$$

where $B_{LL}^{(th)}(r)$ and $B_{NN}^{(th)}(r)$ are obtained from (7.8) by a direct averaging

$$B_{LL}^{(th)}(r) = \langle u_{n_\theta,1}^{det}(r, 0, 0) u_{n_\theta,1}^{det}(0, 0, 0) \rangle, \quad B_{NN}^{(th)}(r) = \langle u_{n_\theta,2}^{det}(r, 0, 0) u_{n_\theta,2}^{det}(0, 0, 0) \rangle. \quad (7.10)$$

Here $u_{n_\theta,i}^{det}$, $i = 1, 2, 3$ are components of the vector $\mathbf{u}_{n_\theta}^{det}$. When evaluating these functions, we substitute the values of the field $\mathbf{u}_{n_\theta}^{det}(\mathbf{x})$ from (7.8) in the right hand side of the last

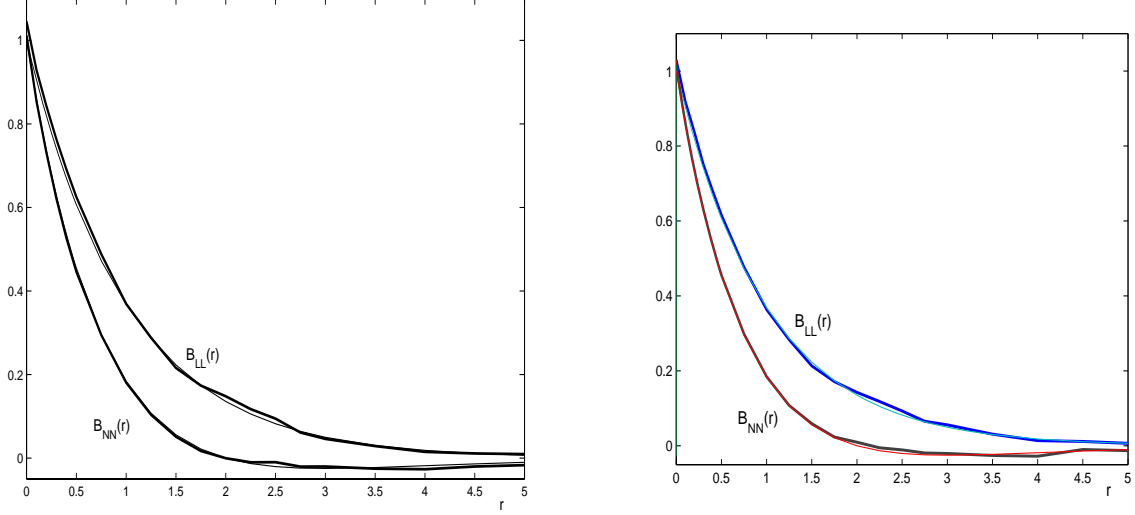


Figure 3: The longitudinal (B_{LL}) and transversal (B_{NN}) correlation functions calculated by RSM (model (7.4) with $n_0 = 25$, left panel), and FWM (model (7.7) with $N_s = 25$, right panel) models through ensemble averaging. Calculations: bold solid line; Explicit result (see (7.2)) : solid line. The number of MC samples in both cases was 16000.

equalities. Then, by the independence of the random processes $\mathbf{v}^{(jr)}(t)$ (for different pairs (j, r) , and for the components $v_l^{(jr)}(t)$, $l = 1, 2, 3$ as well):

$$\langle u_{n_\theta, i}^{det}(r, 0, 0) u_{n_\theta, i}^{det}(0, 0, 0) \rangle = \sum_{j, r} \frac{|\Delta \Omega_{j, r}|}{4\pi} (1 - (\Omega_{j, r}^{(i)})^2) \langle v_i^{(jr)}(r \Omega_{j, r}^{(1)}) v_i^{(jr)}(0) \rangle, \quad i = 1, 2, 3;$$

where $\Omega_{j, r}^{(i)}$, $i = 1, 2, 3$ are components of the vector $\Omega_{j, r}$. The correlation function $B_v(\tau) = \langle v_i^{(jr)}(\tau) v_i^{(jr)}(0) \rangle = \int e^{i2\pi\kappa\tau} E(\kappa) d\kappa$ in the right hand side of the last equality is calculated using FWM $B_v^{(FW)}(\tau)$ presented in (5.12), and in the calculation of $\mathcal{F}_m^{(\phi)}$ and $\mathcal{F}_m^{(\psi)}$ we use the spectral function $Q(k) = E^{1/2}(k)$.

n_θ	4	6	8	10	16	30
N_s	20	44	78	124	320	1132
ϵ_{LL}	0.1055	0.0750	0.0434	0.0190	0.0135	0.0139
ϵ_{NN}	0.0513	0.0365	0.0223	0.0152	0.0146	0.0143

Table 2: Dependence of errors ϵ_{LL} and ϵ_{NN} on n_θ .

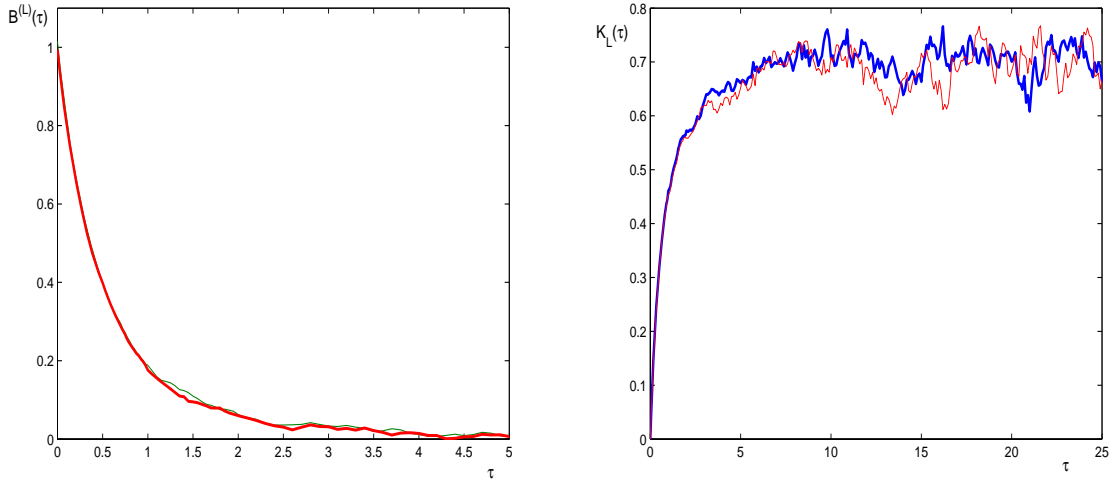


Figure 4: Lagrangian correlation function $B^{(L)}$ (left panel) and the diffusion coefficient K_L (right panel) calculated by RSM (7.4) and FWM (7.7) through ensemble averaging with the same parameters as in Figure 3. Bold solid line - RSM; solid line - FWM.

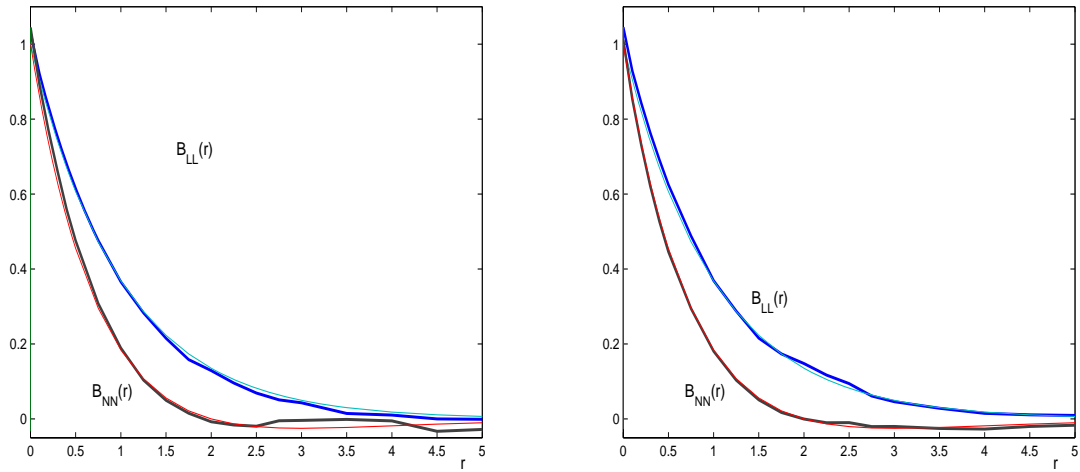


Figure 5: Eulerian longitudinal and transversal correlation functions calculated by RSM (7.4) with $n_0 = 3$ (left panel) and $n_0 = 50$ (right panel). Bold solid line - calculations, solid line - explicit result.

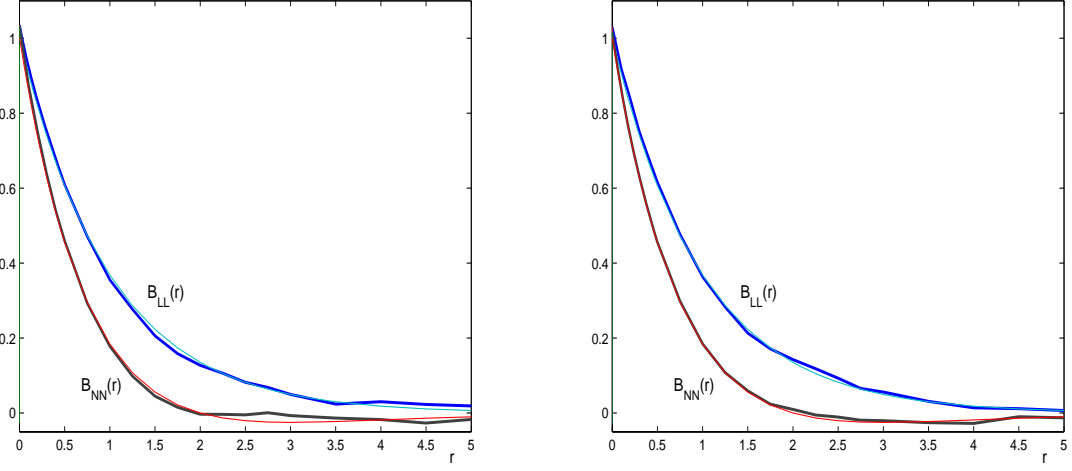


Figure 6: The Eulerian longitudinal and transversal correlation functions calculated by FWM (7.7) with $N_s = 10$ (left panel) and $N_s = 100$ (right panel). Bold solid line - calculations, solid line - explicit result.

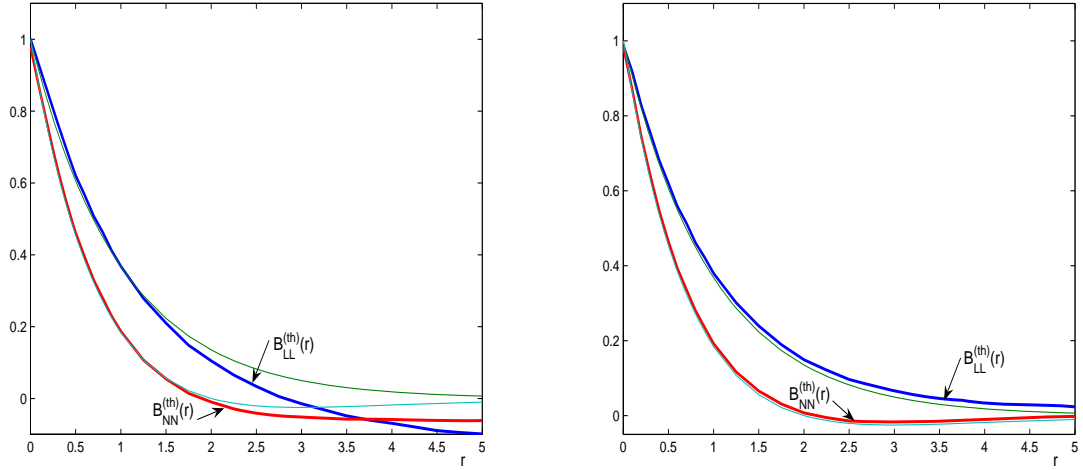


Figure 7: Eulerian longitudinal ($B_{LL}^{(th)}$) and transversal ($B_{NN}^{(th)}$) correlation functions (bold solid lines) for FWM (7.8) with $n_\theta = 4$ (left panel) and $n_\theta = 10$ (right panel); solid lines - explicit results (7.2).

7.4 Space averaging

In this section we deal with the space averaging aiming at evaluating the statistical characteristics of interest (e.g., Eulerian and Lagrangian correlation functions) on the basis of the ergodic property.

Let us discuss this in more details.

Assume we need to evaluate the Eulerian correlation function $B_{LL}(r)$ using only one sample of the random field $\mathbf{u}(\mathbf{x})$. Since $\mathbf{u}(\mathbf{x})$ is homogeneous, the random process $\xi(x; r) = u_1(x+r, 0, 0)u_1(x, 0, 0)$, $x \in \mathbb{R}$ (r is fixed) is stationary, and by definition, $\langle \xi(x; r) \rangle = B_{LL}(r)$. Assuming that this process is ergodic (this is true under quite general conditions, e.g., see [44]) we can evaluate $\langle \xi(x; r) \rangle$ by a spatial averaging. In particular, $\langle \xi(x; r) \rangle \simeq \frac{1}{n_x} \sum_{i=1}^{n_x} \xi(x_i)$, where $x_i, i = 1, \dots, n_x$ is a set of points in \mathbb{R} . It is reasonable to choose the points so that the minimal distance between the points were larger than the characteristic correlation length of our random process $\xi(x; r)$. These arguments can be extended to the case of points $\mathbf{x}_i \in \mathbb{R}^3$ which leads to the relations

$$B_{LL}(r) \simeq \frac{1}{n_p} \sum_{i_x=-n_x}^{n_x} \sum_{i_y=-n_y}^{n_y} \sum_{i_z=-n_z}^{n_z} u_1(i_x L + r, i_y L, i_z L) u_1(i_x L, i_y L, i_z L),$$

$$B_{NN}(r) \simeq \frac{1}{n_p} \sum_{i_x=-n_x}^{n_x} \sum_{i_y=-n_y}^{n_y} \sum_{i_z=-n_z}^{n_z} u_2(i_x L + r, i_y L, i_z L) u_2(i_x L, i_y L, i_z L),$$

where $L > 0$ is the grid size, $n_p = (2n_x + 1)(2n_y + 1)(2n_z + 1)$; in calculations we have taken $n_x = n_y = n_z = 7$ (hence the number of points $n_p = 3375$), and $L = 5$.

Suppose we have to evaluate a Lagrangian characteristics, say, $B_{ij}^{(L)}(t)$, using only one sample of the random field $\mathbf{u}(\mathbf{x})$. Let $\mathbf{X}(t; \mathbf{x}_0)$ be a Lagrangian trajectory starting at a point \mathbf{x}_0 (i.e., a solution to (7.3)). If we take a family of trajectories $\mathbf{X}(t; \mathbf{x}_0^{(i_p)})$, $i_p = 1, \dots, n_p$ starting at the points $\mathbf{x}_0^{(i_p)}$, $i_p = 1, \dots, n_p$, then (under the condition that the minimal distance between these points is sufficiently large so that the different trajectories were possibly small correlated) for sufficiently large values of n_p we can write

$$B_{ij}^{(L)}(t) \simeq \frac{1}{n_p} \sum_{i_p=1}^{n_p} u_i(\mathbf{X}(t; \mathbf{x}_0^{(i_p)})) u_j(\mathbf{x}_0^{(i_p)})$$

$$K_L(t) = \frac{1}{3} \langle (X_i(t) - x_{0,i}) u_i(\mathbf{X}(t)) \rangle \simeq \frac{1}{3n_p} \sum_{i_p=1}^{n_p} (X_i(t; \mathbf{x}_0^{(i_p)}) - x_{0,i}^{(i_p)}) u_i(\mathbf{X}(t; \mathbf{x}_0^{(i_p)})) .$$

We recall that we use the summation convention over the repeated indices.

In the calculations, we have taken the set of starting points as $n_p = (2n_x + 1)(2n_y + 1)(2n_z + 1)$ points: $(i_x L, i_y L, i_z L)$, $i_x = -n_x, \dots, n_x$; $i_y = -n_y, \dots, n_y$; $i_z = -n_z, \dots, n_z$, with $L = 5$, $n_p = 3375$.

In Figures 8-9 the correlation functions $B_{LL}(r)$ and $B_{NN}(r)$ evaluated by RSM (7.4) for different values of n_0 are presented. These results show that to reach the accuracy compared to that of the ensemble averaging calculations, (see Figure 3, left panel) even

$n_0 = 1200$ cannot be considered as satisfied. Close results were obtained by the model (7.6) for $n_\theta \leq 30$ (i.e., $N_s \leq 1132$).

In Figure 10 we plot the functions $B_{LL}(r)$ and $B_{NN}(r)$ calculated by the use of models (7.7) (left panel) and (7.9) (right panel). The model (7.8) with $n_\theta = 10$ gave approximately the same results. The amount of statistics is $n_p = 15^3 = 3375$, so we see that the results are in a good agreement with the results of Figure 3 obtained through the ensemble averaging (note that the statistics in Figure 10 is about 4 times less than that of Figure 3).

Thus we conclude that to calculate the Eulerian correlation functions $B_{LL}(r)$ and $B_{NN}(r)$ by the space averaging with one sample of the field $\mathbf{u}(\mathbf{x})$, the number of harmonics N_s in RSMs (7.4), (7.6) should be taken about several of thousands, to attain the same accuracy as FWMs provide with several of hundreds of harmonics. (in both methods, statistics was 3375).

In Figure 11 the Lagrangian correlation function $B^{(L)}(t) = \frac{1}{3}B_{ii}^{(L)}(t)$ (left panel) and the diffusion coefficient $K_L(t)$ (right panel) was calculated through a space averaging over $n_p = 3375$ Lagrangian trajectories, by RSM (7.6) and FW model (7.8) with $n_\theta = 10$. For comparison, we show also the results obtained through the ensemble averaging by RSM (7.4) with $n_0 = 25$. Note that when calculating Lagrangian statistical characteristics by averaging over Lagrangian trajectories in one fixed sample, the RSM and FWM have approximately the same efficiency. In this case, the number of harmonics in FWM and RSM can be taken about of several hundreds.

In Figures 12, 13 we plot the Eulerian conditional correlation functions $B_{LL}^{(th)}(r)$ and $B_{NN}^{(th)}(r)$ of the random fields (7.7) and (7.8) calculated by ensemble averaging over the processes $\mathbf{v}^{(jr)}(t)$, for fixed $\boldsymbol{\omega}_{j,r}$ and $\boldsymbol{\Omega}_{jr}$, respectively. These functions are calculated according FWM (7.7) analogously to the above discussed case (7.10)). These plots show that for relatively large values, $N_s \simeq 100$, it is better to use the stratified model (7.8), than the simpler model (7.7) with independent isotropically distributed random nodes $\boldsymbol{\omega}_i$. As to the hybrid model (7.9), it gave (for $N_s \geq 100$) practically the same results as that of the model (7.8).

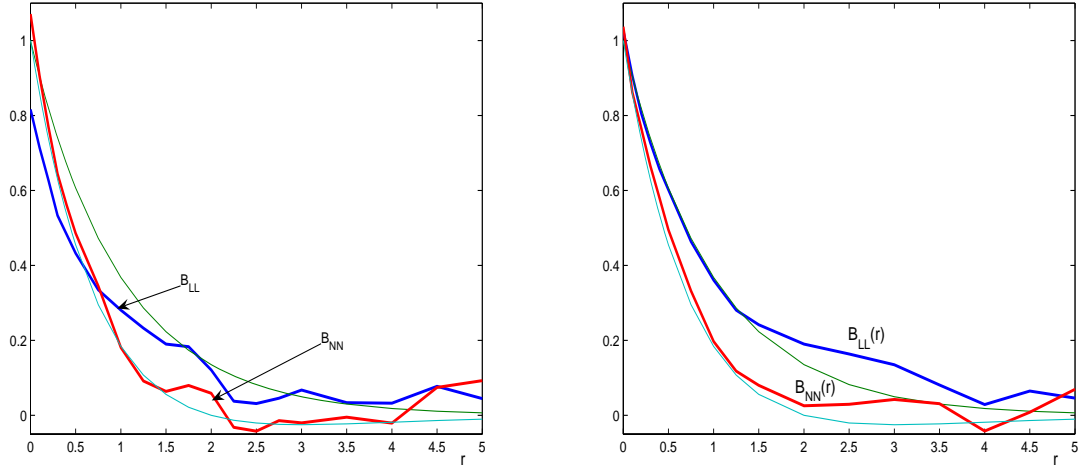


Figure 8: Eulerian longitudinal and transversal correlation functions calculated by RSM (7.4) with $n_0 = 100$ (left panel) and $n_0 = 400$ (right panel) obtained by space averaging. Bold solid line - calculations, solid line - explicit result.

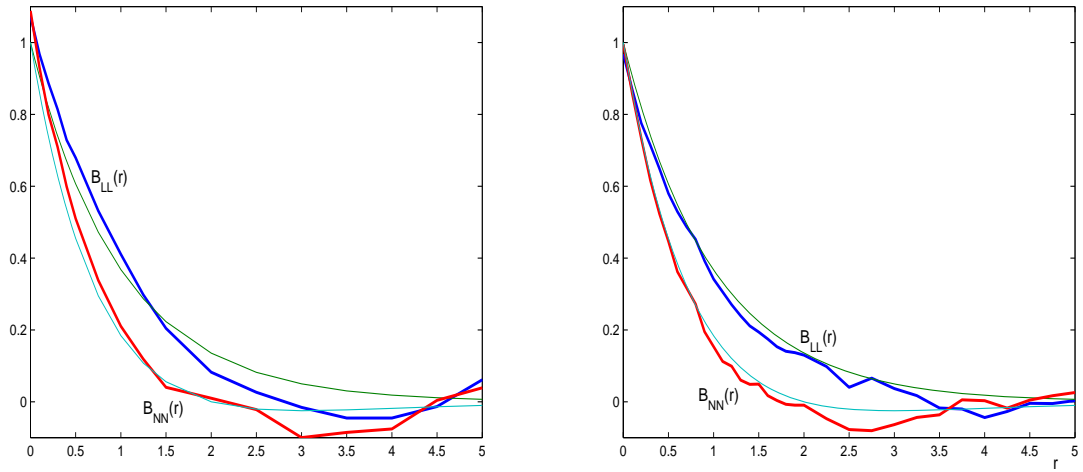


Figure 9: Eulerian longitudinal and transversal correlation functions calculated by RSM (7.4) with $n_0 = 800$ (left panel) and $n_0 = 1200$ (right panel) obtained by space averaging. Bold solid line - calculations, solid line - explicit result.

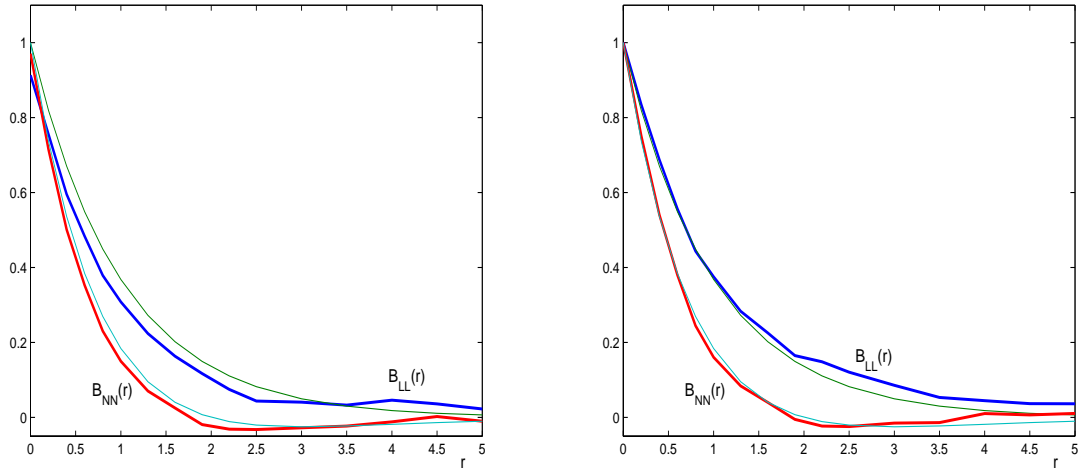


Figure 10: Eulerian longitudinal and transversal correlation functions calculated by FWM (7.7) with $Ns = 200$ (left panel) and (7.9) with $n_\theta = 10$ (right panel) obtained by space averaging. Bold solid line - calculations, solid line - explicit result.

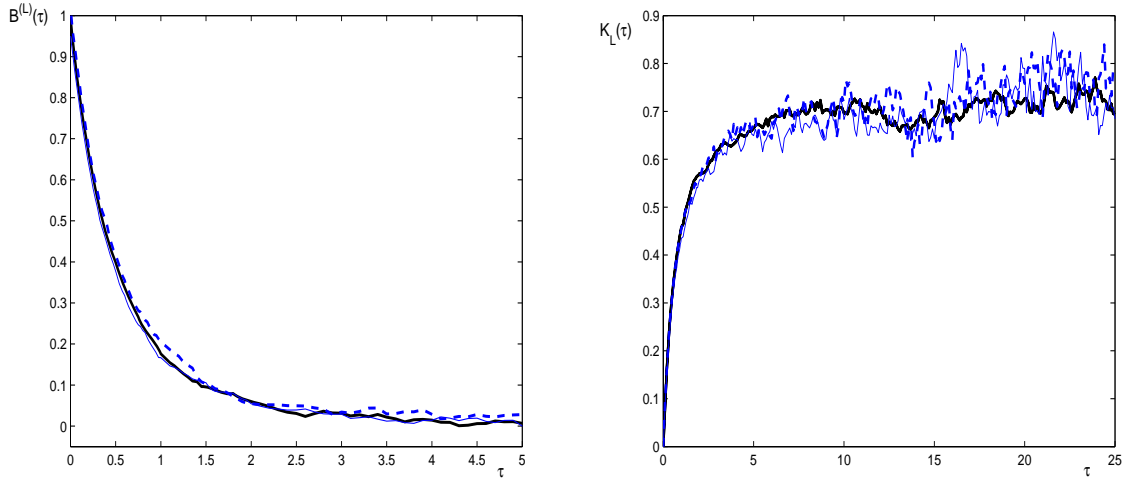


Figure 11: The Lagrangian correlation functions (left panel) and the diffusion coefficient (right panel) calculated by RSM (7.6) and FWM (7.8) averaged over 3375 Lagrangian trajectories. Bold solid line - ensemble averaging by RSM with $n_0 = 25$, bold dashed line - trajectory averaged by RSM (7.6) with $n_\theta = 10$; solid line - FWM (7.8) with $n_\theta = 10$.

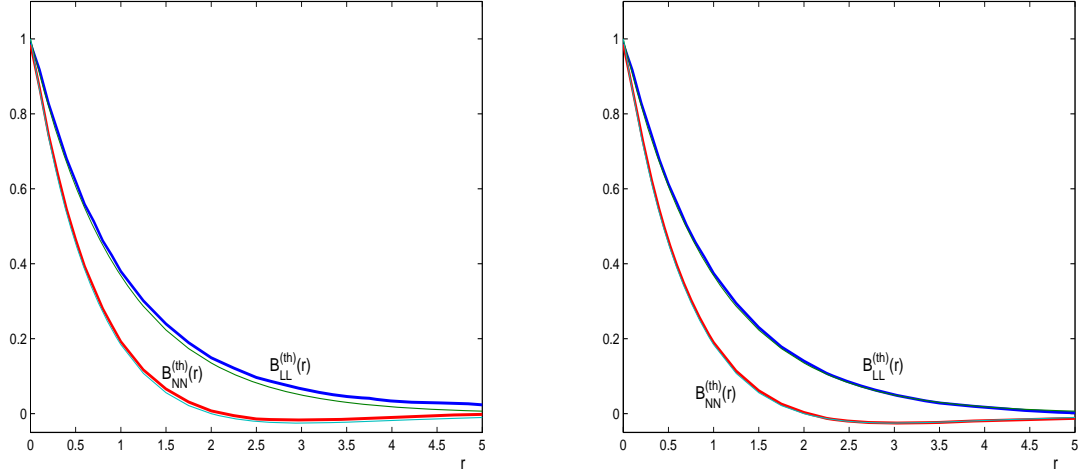


Figure 12: The Eulerian correlation functions $B_{LL}^{(th)}$ and $B_{NN}^{(th)}$ for the model(7.8) with $n_\theta = 10$ (left panel) and $n_\theta = 16$ (right panel). Bold solid line - calculations, solid line - explicit result.

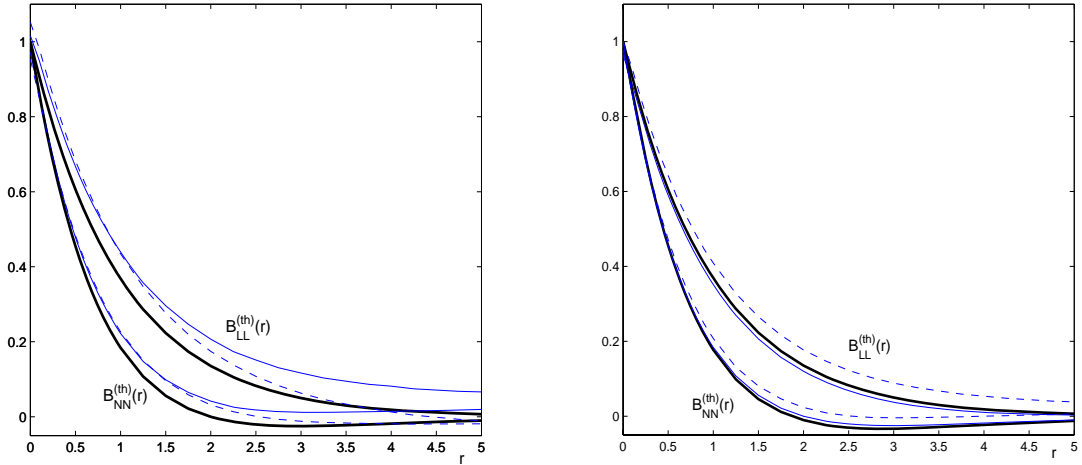


Figure 13: The conditional Eulerian correlation functions $B_{LL}^{(th)}$ and $B_{NN}^{(th)}$ (solid and dashed lines) for the model(7.7) with $N_s = 100$ (left panel) and $N_s = 200$ (right panel) for two realizations of $\{\omega_i\}_{i=1}^{N_s}$. Bold solid lines - explicit result.

Conclusion.

Simulation methods of homogeneous Gaussian random fields based on randomized spectral representations and Fourier-Wavelet decomposition are presented. Extensions of Fourier-Wavelet Method (FWM) from scalar processes and isotropic fields to general vector fields are suggested. Convergence of the constructed Fourier-Wavelet models (in the sense of finite-dimensional distributions) under some general conditions on the spectral tensor is given. A comparative analysis of RSM and FWM is made by calculating Eulerian and Lagrangian statistical characteristics of a 3D isotropic incompressible random field through an ensemble and space averaging.

The comparative analysis can be summarized as follows;

- In the case of ensemble averaging, in contrast to the one-dimensional case, the complexity of Randomized Spectral Model (RSM) and 3D FWM are more or less compatible because in FWM based on the plane-wave decomposition, the one-dimensional processes are precalculated on a fine grid in advance so that there is no need in the sophisticated management of random numbers choice. The best results are obtained when the number of one-dimensional processes is about 10. Nevertheless, the RSM seem to be preferable in this case since its implementation is much easier.
- For space averaging, when evaluating Eulerian characteristics using one sample of the simulated random field, FWM shows higher efficiency because its samples have better ergodic properties. To get stable results by RSM, one needs a huge number (several thousands) of harmonics.
- When calculating Lagrangian statistical characteristics by averaging over Lagrangian trajectories in one fixed sample, the RSM and FWM have approximately the same efficiency. In this case, the number of harmonics in FWM and RSM can be taken about of several hundreds. Here a stratification in the directional space improves the results considerably.

8 Appendix A: Positive definiteness of the matrix \mathcal{B}

Here we prove that the matrix \mathcal{B} with entries (6.3) is positive definite, i.e., for any N -dimensional vector-rows $\mathbf{c}_1, \dots, \mathbf{c}_N \in \mathbb{R}^m$

$$\mathbf{c}_i b_{ij} \mathbf{c}_j^T = \int_{A_i \cap A_j} \mathbf{c}_i B(t_i - t_j; \boldsymbol{\Omega}) \mathbf{c}_j^T d\boldsymbol{\Omega} \geq 0 \quad (8.1)$$

is true for all integers $N > 0$ and values t_1, \dots, t_N in \mathbb{R} , and measurable subsets A_1, \dots, A_N in S_{d-1} .

Let $\{\mathcal{D}_\alpha\}_{\alpha=1}^M$ be a subdivision of the set $A = \cup_{i=1}^N A_i$ (i.e., $\mathcal{D}_\alpha \cap \mathcal{D}_\beta = \emptyset$ if $\alpha \neq \beta$, and $A = \cup_{\alpha=1}^M \mathcal{D}_\alpha$) such that it is also a subdivision of A_i for any $i = 1, \dots, N$: $A_i = \cup_{\alpha_j=1}^{N_i} \mathcal{D}_{\alpha_j}$. Let $\mathbf{u}_\alpha(t)$, $1 \leq \alpha \leq M$ be a family of n -dimensional vector-columns, mutually independent, zero mean Gaussian random processes with the correlation tensor $\int_{\mathcal{D}_\alpha} B(t, \boldsymbol{\Omega}) d\boldsymbol{\Omega}$. Let us

construct, for each $i = 1, \dots, N$, a zero mean Gaussian random process $\mathbf{v}_i(t)$ by putting $\mathbf{v}_i(t) = \sum_{j=1}^{N_i} \mathbf{u}_{\alpha_j}(t)$. Then obviously,

$$\langle \mathbf{v}_i(t) \mathbf{v}_j^T(t) \rangle = \int_{A_i \cap A_j} B(t_i - t_j; \boldsymbol{\Omega}) d\boldsymbol{\Omega}.$$

Introducing a random variable $\xi = \mathbf{c}_i \mathbf{v}_i(t_i)$ (here we recall about the summation convention) yields

$$\langle \xi^2 \rangle = \langle \mathbf{c}_i \mathbf{v}_i \mathbf{v}_j^T \mathbf{c}_j^T \rangle = \mathbf{c}_i b_{ij} \mathbf{c}_j^T.$$

which ensures (8.1).

9 Appendix B: Proof of the Proposition 1

From the definition (5.10) we have for the random field $u^{(FW)}$:

$$u(x) = u^{(FW)}(x) + \delta v_{m_0}^{(1)}(x) + \sum_{m=m_0}^{m_1} \delta v_m^{(2)}(x) + \delta v_{m_1}^{(3)}(x), \quad (9.1)$$

where

$$\begin{aligned} \delta v_{m_0}^{(1)}(x) &= \sum_{j: |j - \lfloor 2^{m_0} x \rfloor| > b_0} \mathcal{F}_{m_0}^{(\phi)}(2^{m_0} x + j) \xi_j \\ \delta v_m^{(2)}(x) &= \sum_{j: |j - \lfloor 2^m x \rfloor| > b_1} \mathcal{F}_m^{(\psi)}(2^m x + j) \xi_{mj} \\ \delta v_{m_1}^{(3)}(x) &= \sum_{m=m_1+1}^{\infty} \sum_{j=-\infty}^{\infty} \mathcal{F}_m^{(\psi)}(2^m x + j) \xi_{mj}. \end{aligned}$$

The random variables ξ_j, ξ_{mj} are mutually independent, hence the terms in the right hand side of (9.1) are also independent, therefore

$$\begin{aligned} \langle u(x+r)u(x) \rangle - \langle u^{(FW)}(x+r)u^{(FW)}(x) \rangle &= \langle \delta v_{m_0}^{(1)}(x+r)\delta v_{m_0}^{(1)}(x) \rangle \\ &+ \sum_{m=m_0}^{m_1} \langle \delta v_m^{(2)}(x+r)\delta v_m^{(2)}(x) \rangle + \langle \delta v_{m_1}^{(3)}(x+r)\delta v_{m_1}^{(3)}(x) \rangle. \end{aligned} \quad (9.2)$$

Let us estimate the terms in the right hand side. First, we have for the last term

$$|\langle \delta v_{m_1}^{(3)}(x+r)\delta v_{m_1}^{(3)}(x) \rangle| \leq (\langle (\delta v_{m_1}^{(3)}(x+r))^2 \rangle \langle (\delta v_{m_1}^{(3)}(x))^2 \rangle)^{1/2}. \quad (9.3)$$

Lemma 1. Assume that for some $s > 0$

$$I_s = \int_{-\infty}^{\infty} F(k)(1 + |k|^2)^s dk < \infty. \quad (9.4)$$

Then a constant B_s depending only on s can be found such that

$$\langle (\delta v_{m_1}^{(3)}(x))^2 \rangle \leq \frac{B_s^2}{4^{(m_1+1)s}} \int_{-\infty}^{\infty} F(k)(1+|k|^2)^s dk. \quad (9.5)$$

Proof. Note that

$$\langle (\delta v_{m_1}^{(3)}(x))^2 \rangle = \sum_{m=m_1+1}^{\infty} \sum_{j=-\infty}^{\infty} |\mathcal{F}_m^{(\psi)}(2^m x + j)|^2. \quad (9.6)$$

Further, by (3.9)

$$\mathcal{F}_m^{(\psi)}(2^m x + j) = G_{mj}^{(\psi)}(x) = \int_{-\infty}^{\infty} e^{i2\pi kx} Q(k) \bar{\psi}_{mj}(k) dk = \int_{-\infty}^{\infty} G(x+y) \psi_{mj}(y) dy$$

where $G(x) = \int_{-\infty}^{\infty} e^{i2\pi kx} Q(k) dk$. Consequently for fixed x , the quantities $\mathcal{F}_m^{(\psi)}(2^m x + j)$ ($m, j = \dots, -1, 0, 1, \dots$) are Fourier coefficients in the expansion of $G(x + \cdot)$ with respect to orthonormal system ψ_{mj} ($m, j = \dots, -1, 0, 1, \dots$). Notice that the condition (9.4) can be formulated equivalently that the function G belongs to the space of Bessel potentials $H_2^s(\mathbb{R})$ (since $G \in H_2^s(\mathbb{R})$ means that the function $Q(k)(1+|k|^2)^{s/2}$ is from $L_2(\mathbb{R})$) and $\|G\|_{H_2^s} = I_s^{1/2}$ (more details in [42])). Further we use the fact that $H_2^s(\mathbb{R})$ coincides with the Besov space $B_{22}^s(\mathbb{R})$, and the norms in these spaces are equivalent (see [42], section 2.3.9). On the other hand, it is known(see [30]), that under quite general assumptions on the wavelet function $\psi(x)$ (Meyer's wavelet function satisfies this condition if the function $\nu(x)$ is smooth enough) the norm $\|f\|_{B_{pq}^s}$ in Besov's space $B_{pq}^s(\mathbb{R})$, $1 \leq p, q \leq \infty$, $s > 0$ can be equivalently defined through the wavelet coefficients $\beta_{mj} = \int f(x) \psi_{mj}(x) dx$ by

$$\|f\|_{B_{pq}^s} = \|f\|_{L_p} + \left\{ \sum_{m=-\infty}^{\infty} \left(\sum_{j=-\infty}^{\infty} (|\beta_{mj}| 2^{m(s+\frac{1}{2}-\frac{1}{p})})^p \right)^{q/p} \right\}^{1/q}.$$

Since $G \in B_{22}^s$, we conclude

$$\sum_{m=-\infty}^{\infty} \sum_{j=-\infty}^{\infty} |\mathcal{F}_m^{(\psi)}(2^m x + j)|^2 4^{ms} \leq B_s^2 \|G(x + \cdot)\|_{H_2^s}^2$$

for some B_s depending only on s . From this we get by $\|G(x + \cdot)\|_{H_2^s}^2 = \|G\|_{H_2^s}^2 = I_s$ that

$$\sum_{m=m_1+1}^{\infty} \sum_{j=-\infty}^{\infty} |\mathcal{F}_m^{(\psi)}(2^m x + j)|^2 \leq \sum_{m=m_1+1}^{\infty} \sum_{j=-\infty}^{\infty} |\mathcal{F}_m^{(\psi)}(2^m x + j)|^2 \frac{4^{ms}}{4^{(m_1+1)s}} \leq \frac{B_s^2}{4^{(m_1+1)s}} I_s.$$

This completes the proof.

This implies due to (9.3) and (9.5) that the last term in the right hand side of (9.2) can be estimated as follows:

$$|\langle \delta v_{m_1}^{(3)}(x+r) \delta v_{m_1}^{(3)}(x) \rangle| \leq \frac{B_s^2}{4^{(m_1+1)s}} \int_{-\infty}^{\infty} F(k)(1+|k|^2)^s dk. \quad (9.7)$$

Now we turn to the estimation of the first two terms in the right hand side of (9.2). We will use some results from the theory of Nikolskiĭ-Besov spaces (e.g., see [33], [42]).

A triple (r, j, l) is called admissible if $j \in \mathbb{N}$, $l \in \mathbb{N}_0$ and $j > r - l$. Here $\mathbb{N}_0 = \{0, 1, 2, \dots\}$ and $\mathbb{N} = \{1, 2, \dots\}$. Let us denote by $\Delta_h^{(j)} g$ the j -th difference of g :

$$\Delta_h g(\cdot) = g(\cdot + h) - g(\cdot), \dots, \Delta_h^{(j)} g(\cdot) = \Delta_h \Delta_h^{(j-1)} g(\cdot).$$

For $1 \leq p, q \leq \infty$, $r > 0$ the space $B_{pq}^r(\mathbb{R})$ consists of all functions f such that the norm

$$\|f\|_{B_{pq}^r} = \|f\|_{L_p} + \|f\|_{b_{pq}^r},$$

where

$$\|f\|_{b_{pq}^r} = \left(\int_{-1}^1 \left(\frac{\|\Delta_h^{(j)} f^{(l)}\|_{L_p}}{|h|^{r-l}} \right)^q \frac{dh}{|h|} \right)^{\frac{1}{q}}, \quad 1 \leq q < \infty, \quad (9.8)$$

$$\|f\|_{b_{p\infty}^r} = \sup_{0 < |h| \leq 1} |h|^{l-r} \|\Delta_h^{(j)} f^{(l)}\|_{L_p} \quad (9.9)$$

makes sense and is finite for some admissible triple (r, j, l) . The ambiguity in the choice of triple (r, j, l) is not essential: different admissible triples correspond to equivalent norms.

We will exploit the following imbeddings (e.g., see [33], [42]):

$$B_{pq}^r(\mathbb{R}) \hookrightarrow B_{p_1q}^\rho(\mathbb{R}), \quad \rho = r \left(1 - \frac{1}{r} \left(\frac{1}{p} - \frac{1}{p_1} \right) \right), \quad 1 \leq p < p_1 < \infty, \quad (9.10)$$

$$B_{p\infty}^{r+\varepsilon}(\mathbb{R}) \hookrightarrow B_{pq}^r(\mathbb{R}) \hookrightarrow B_{p_1q_1}^r(\mathbb{R}), \quad 1 \leq q < q_1 \leq \infty, \quad \varepsilon > 0, \quad (9.11)$$

$$B_{p_1}^l(\mathbb{R}) \hookrightarrow W_p^l(\mathbb{R}) \hookrightarrow B_{p\infty}^l(\mathbb{R}), \quad l \in \mathbb{N}_0, \quad 1 \leq p < \infty, \quad (9.12)$$

$$B_{pp}^l(\mathbb{R}) \hookrightarrow W_p^l(\mathbb{R}) \hookrightarrow B_{pp}^l(\mathbb{R}), \quad l \in \mathbb{N}_0, \quad 1 \leq p < \infty, \quad (9.13)$$

where $W_p^l(\mathbb{R})$ is the Sobolev space, and $X \hookrightarrow Y$ for seminormed spaces X and Y means that $X \subset Y$ and there exists a constant $c > 0$ such that the inequality $\|x\|_Y \leq c\|x\|_X$ is fulfilled.

Lemma 2. Let $\hat{f} \in B_{1\infty}^r(\mathbb{R})$, $r > 1/2$. Then f is uniformly continuous, $f \in L_2(\mathbb{R})$ and there exists a positive constant C_r depending only on r such that for all $x \in \mathbb{R}$

$$|x|^r |f(x)| \leq C_r \|\hat{f}\|_{B_{1\infty}^r}. \quad (9.14)$$

Proof. The uniform continuity of f follows from the fact that $\hat{f} \in L_1(\mathbb{R})$ since $B_{1\infty}^r(\mathbb{R}) \subset L_1(\mathbb{R})$. Then, for a positive $\varepsilon \in (0, r - 1/2)$ in view of (9.10) and (9.11)

$$B_{1\infty}^r(\mathbb{R}) \hookrightarrow B_{2\infty}^{r-1/2}(\mathbb{R}) \hookrightarrow B_{22}^{r-1/2-\varepsilon}(\mathbb{R}). \quad (9.15)$$

From this we get by (9.13) that $\hat{f} \in L_2(\mathbb{R})$, hence $f \in L_2(\mathbb{R})$. Let' $l = \lfloor r \rfloor$ be the integer part of r . From

$$\Delta_h^{(l+2)} \hat{f}(k) = \int_{-\infty}^{\infty} e^{-i2\pi kx} (e^{-i2\pi hx} - 1)^{l+2} f(x) dx \quad (9.16)$$

and $f \in L_2(\mathbb{R})$ it follows by the inverse Fourier transform

$$f(x)(e^{-i2\pi hx} - 1)^{l+2} = \int_{-\infty}^{\infty} e^{i2\pi kx} \Delta_h^{(l+2)} \hat{f}(k) dk. \quad (9.17)$$

Taking the absolut values and dividing this equation by $|h|^r$ we then take the supremum over $h \in \mathbb{R}$. This yields

$$|x|^r |f(x)| C'_r \leq \sup_{h \in \mathbb{R}} |h|^{-r} \|\Delta_h^{(l+2)} \hat{f}\|_{L_1}, \quad (9.18)$$

where

$$C'_r = \sup_{t \in \mathbb{R}} \left\{ \frac{|e^{-i2\pi t} - 1|^{l+2}}{|t|^r} \right\}. \quad (9.19)$$

Since the triple $(r, l + 2, 0)$ is admissible, and $\sup_{h \in \mathbb{R}} |h|^{-r} \|\Delta_h^{(l+2)} \hat{f}\|_{L_1} \leq C''_r \|\hat{f}\|_{B_{1\infty}^r}$ for some C''_r depending only on r , the proof of Lemma 2 is complete.

To get an estimation for $\langle \delta v_{m_0}^{(1)}(x+r) \delta v_{m_0}^{(1)}(x) \rangle$ we estimate the quantity

$$\langle (\delta v_{m_0}^{(1)}(x))^2 \rangle = \sum_{j: |j - \lfloor 2^{m_0} x \rfloor| > b_0} |\mathcal{F}_{m_0}^{(\phi)}(2^{m_0} x + j)|^2. \quad (9.20)$$

We first estimate each term of this sum. The function $\mathcal{F}_m^{(\phi)}(y)$ has the Fourier transform $2^{m/2} Q(2^m k) \hat{\phi}(k)$ (see (3.8)). Hence if $\hat{\phi}$ is smooth enough and if the function $Q(k)$ belongs to the Nikolskii-Besov space $B_{1\infty}^\rho(\mathbb{R})$, $\rho > 1/2$, then $2^{m/2} Q(2^m k) \hat{\phi}(k) \in B_{1\infty}^\rho(\mathbb{R})$. Then from (9.14) we get

$$|\mathcal{F}_m^{(\phi)}(y)| \leq \frac{C_\rho}{|y|^\rho} \|2^{m/2} Q(2^m \cdot) \hat{\phi}\|_{B_{1\infty}^\rho} = \frac{C_{\rho m}(\phi, Q)}{|y|^\rho}, \quad (9.21)$$

where $C_{\rho m}(\phi, Q)$ is a constant depending on ρ , m and functions ϕ and Q . Note that from (9.20) and (9.21) we get

$$\langle (\delta v_{m_0}^{(1)}(x))^2 \rangle \leq \frac{C'_{ml}}{b_0^{2\rho-1}}.$$

The same arguments can be used to estimate the terms in the right hand side of (9.2) related with $\delta v_m^{(2)}$.

Thus, the proof of the Proposition 2 is complete.

References

- [1] Buglanova N.A. and Kurbanmuradov O. Convergence of the Randomized Spectral Models of Homogeneous Gaussian Random Fields. *Monte Carlo Methods and Appl.*, vol. 1, No-3, 173-201, 1995.
- [2] Chris Cameron. Relative efficiency of Gaussian stochastic process sampling procedures. *J. Comput. Phys.*, 192(2):546–569, 2003.
- [3] Charles K.Chui. *An Introduction to Wavelets*. Academic Press, Inc., 1992.
- [4] G. Dagan. Flow and Transport in Porous Formations. Springer-Verlag, Berlin-Heidelberg, Germany, 1989.
- [5] G. Dagan. Spatial moments, Ergodicity, and Effective Dispersion. *Water Resour. Res.*, **26**, No. 6, 1990, 1281-1290.
- [6] I.Daubechies. *Ten Lectures On Wavelets*. CBS-NSF Regional Conferences in Applied Mathematics, **61**, SIAM, 1992
- [7] G. Deodatis and M. Shinozuka. Simulation of stochastic processes by spectral representation. Applied Mechanics Reviews, **44**, No.4, 1991, 191-204.
- [8] M.W. Davis, Production of conditional simulations via the LU trangular decomposition of the covariance matrix, *Math. Geol.*, **19**, 1987, 91-98.
- [9] C.R. Dietrich and G.N. Newsam. Fast and Exact Simulation of Stationary Gaussian Processes through Circulant Embedding of the Covariance Matrix, *Siam J. Sci. Comput.*, **18**, No. 4, 1997, 1088-1107.
- [10] Frank W. Elliott, Jr, David J. Horntrop, and Andrew J. Majda. A Fourier-wavelet Monte Carlo method for fractal random fields. *J. Comp. Phys*, 132(2):384–408, 1997.
- [11] Frank W. Elliott, Jr, David J. Horntrop, and Andrew J. Majda. Monte Carlo methods for turbulent tracers with long range and fractal random velocity fields. *Chaos*, 7(1):39–48, 1997.
- [12] Frank W. Elliott, Jr and Andrew J. Majda. A wavelet Monte Carlo method for turbulent diffusion with many spatial scales. *J. Comp. Phys*, 113(1):82–111, July 1994.
- [13] Frank W. Elliott, Jr and Andrew J. Majda. A new algorithm with plane waves and wavelets for random velocity fields with many spatial scales. *J. Comp. Phys*, 117:146–162, 1995.
- [14] Frank W. Elliott, Jr and Andrew J. Majda. Pair dispersion over an inertial range spanning many decades. *Phys. Fluids*, 8(4):1052–1060, 1996.
- [15] Fenton, G.A., Error evaluation of three random field generators, *ASCE Journal of Engineering Mechanics*, 120(12), 2487-2497, 1994,

- [16] J. C. H. Fung, J. C. R. Hunt, N. A. Malik, and R. J. Perkins. Kinematic simulation of homogenous turbulence by unsteady random Fourier modes. *J. Fluid Mech.*, 236:281–318, 1992.
- [17] Lynn W. Gelhar. *Stochastic Subsurface Hydrology*. Prentice-Hall, Englewood Cliffs, N.J., 1993.
- [18] Gikhman I.I. and Skorohod A.V. *Introduction to the Theory of Random Processes*. Philadelphia, W.B., Saunders Company, 1969.
- [19] Eugenio Hernandez and Guido Weiss. *A First Course on Wavelets*. CRC Press, Inc., 1996.
- [20] D. Kolyukhin and K. Sabelfeld. Stochastic flow simulation in 3D Porous media. *Monte Carlo Methods and Applications*, **11**, No. 1, 2005, 15-38.
- [21] R.H. Kraichnan. Diffusion by a random velocity field. *Phys.Fluids*, **13** (1970), N1, 22-31.
- [22] Peter R. Kramer. A Review of Some Monte Carlo Simulation Methods for Turbulent Systems. *Monte Carlo Methods and Appl.*, **7**, No. 3-4, 229-244, 2001.
- [23] P. Kramer, O. Kurbanmuradov and K. Sabelfeld. Extensions of multiscale Gaussian random field simulation algorithms. Preprint No. 1040, WIAS, Berlin, 2005.
- [24] Kurbanmuradov O. Weak Convergens of Approximate Models of Random Fields. *Russian Journal of Numerical Analysis and Mathematical Modelling*, **10** (1995), N6, 500-517.
- [25] Kurbanmuradov O. Weak Convergence of Randomized Spectral Models of Gaussian Random Vector Fields. *Bull.Novosibirsk Computing Center, Numerical Analysis*, issue 4, 19-25, 1993.
- [26] O. Kurbanmuradov, K. Sabelfeld, and D. Koluhi. Stochastic Lagrangian models for two-particle motion in turbulent flows. Numerical results. *Monte Carlo Methods Appl.*, 3(3):199–223, 1997.
- [27] Kurbanmuradov O., Sabelfeld K., Smidts O. and Vereecken H.A. Lagrangian stochastic model for transport in statistically homogeneous porous media. *Monte Carlo Methods and Applications*. **9**, No. 4, 2003, 341-366.
- [28] A. Majda. Random shearing direction models for isotropic turbulent diffusion. *J. Stat. Phys.*, **75** (1994), 1153.
- [29] A. McCoy. PhD thesis, University of California at Berkley, 1975
- [30] Y. Meyer. *Ondelettes et opérateurs. I: Ondelettes*, Hermann, Paris, 1990. (English translation: *Wavelets and operators*, Cambridge University Press, 1992.)
- [31] Mikhailov G.A. Approximate models of random processes and fields. *Russian J. Comp. Mathem. and mathem. Physics*, vol.23 (1983), N3, 558-566. (in Russian).

- [32] A.S. Monin and A.M. Yaglom. *Statistical Fluid Mechanics: Mechanics of Turbulence*, Volume 2. The M.I.T. Press, 1981.
- [33] Nikolskiĭ S.M. *Approximation of function of several variables and imbedding theorems*: 2nd edition, Nauka, Moscow, 1977.
- [34] K.K. Phoon, H.W. Huang and S.T. Quek, Comparison between Karhunen-Loeve and wavelet expansions for simulation of Gaussian processes. *Computers and Structures*, **82**, 2004, 985-991.
- [35] F. Poirion and C. Soize. Numerical methods and mathematical aspects for simulation of homogenous and non homogenous Gaussian vector fields. In Paul Kree and Walter Wedig, editors, *Probabilistic methods in applied physics*, volume 451 of *Lecture Notes in Physics*, pages 17–53. Springer-Verlag, Berlin, 1995.
- [36] Karl K. Sabelfeld. *Monte Carlo methods in boundary value problems*, Springer-Verlag, New York, Berlin, 1991.
- [37] M.K. Schneider and A.S. Willsky, A Krylov Subspace Method for Covariance Approximation and Simulation of Random Processes and Fields., *Multidimensional Systems and Signal Processing*, Volume 14 , Issue 4 , 2003, 295-318.
- [38] M. Shinozuka. Simulation of multivariate and multidimensional random processes. *J. of Acoust. Soc. Am.* **49** (1971), 357-368.
- [39] P. Spanos and R. Ghanem, Stochastic finite element expansion for random media. *Journal of Engineering Mechanics, ASCE*, **115**, 1989, 1035-1053.
- [40] P.D. Spanos and V. Ravi S. Rao. Random Field Representation in a Biorthogonal Wavelet Basis. *Journal of Engineering Mechanics*, **127**, No.2 (2001), 194-205.
- [41] D. J. Thomson and B.J. Devenish. Particle pair in kinematic simulations. *Journal of Fluid Mechanics*, **526** (2005), 277-302.
- [42] H. Triebel. *it Theory of function spaces*. Birkhäuser, Basel-Boston-Stuttgart, Akademische Verl. Ges., Leipzig, 1983.
- [43] E. Van Marcke, *Random Fields: Analysis and Synthesis*, The MIT Press, Cambridge (Mass.), 1988.
- [44] A. M. Yaglom. *Correlation theory of stationary and related random functions. Volume I: Basic results*. Springer-Verlag, Berlin, 1987.
- [45] B.A. Zeldin and P.D. Spanos. Random Field Representation and Synthesis Using Wavelet Basis. *ASME Journal of Applied Mechanics*, **63**, (1996), 946-952.